Precambrian Research 231 (2013) 61–77

Contents lists available at SciVerse ScienceDirect

Precambrian Research

journal homepage: www.elsevier.com/locate/precamres

Late Paleoproterozoic sedimentary and mafic rocks in the Hekou area, SW China: Implication for the reconstruction of the Yangtze Block in Columbia

Wei Terry Chen [a], Mei-Fu Zhou [a,*], Xin-Fu Zhao [a,b]

[a] Department of Earth Sciences, University of Hong Kong, Pokfulam Road, Hong Kong, China
[b] Faculty of Earth Resources, China University of Geosciences, Wuhan 430074, China

ARTICLE INFO

Article history:
Received 17 September 2012
Received in revised form 3 February 2013
Accepted 19 March 2013

Keywords:
Hekou Group
Yangtze Block
Zircon
Continental rift
Columbia supercontinent

ABSTRACT

The Paleoproterozoic Hekou Group in the western Yangtze Block is a volcano-sedimentary succession that is intruded by gabbroic plutons. Sedimentary rocks in the group include slates, marble and meta-siltstones interlayered with felsic metavolcanic rocks, metabasalts and metatuffs. Both the volcanic rocks of the Hekou Group and gabbros have undergone upper greenschist to lower amphibolite facies metamorphism. Metatuff samples from different layers have average zircon U-Pb ages of ~1697 Ma, slightly older than the intruding gabbroic plutons with zircon U-Pb ages of ~1684 Ma. Both metabasalts and metagabbros have similar elemental and isotopic compositions, indicative of a co-magmatic origin. They are rich in TiO_2 (mostly >2.5 wt.%), Zr (94.5–347 ppm), Ta (0.48–3.00 ppm) and Th (1.05–7.61 ppm) with high Nb/Y ratios (mostly >0.6) and LREE-enriched chondrite-normalized REE patterns, resembling within-plate mafic rocks. Their positive whole-rock $\varepsilon Nd(t)$ (0.2 to +3.4) and zircon $\varepsilon Hf(t)$ values (−3.3 to +8.4) suggest contributions from a depleted mantle source. The large range of $\varepsilon Nd(t)$ and $\varepsilon Hf(t)$ values, and variable degrees of Nb-Ta anomalies (Ta/La_{PN} = 0.17–1.75) are indicative of crust contamination during magma ascending. Both the metabasalts and metagabbros are considered to have formed in a continental rift setting.

Detrital zircon grains from meta-siltstones in the Hekou Group have U-Pb age populations mainly at 2070–1880 Ma, 2330–2250 Ma and 2900–2700 Ma. These age populations are comparable to those of the North Australian and North China Cratons in the Columbia supercontinent. However, in terms of geochemical features, the ~1.7 Ga within-plate mafic rocks at Hekou are similar to those from the ~1.7 Ga Leichhardt and Calvert Superbasins of the North Australian Craton, but different from those from the 1.7–1.2 Ga Zhaertai-Bayan Obo rift zone of the North China Craton. It is thus suggested that the Yangtze Block was more likely linked with the North Australian Craton in Columbia during the Late Paleoproterozoic. These rifting basins and mafic rocks may record the initial break-up of the Columbia supercontinent.

1. Introduction

The Yangtze Block consists predominantly of Meso- to Neoproterozoic rocks with sparse Archean to Paleoproterozoic rocks (Wan, 2004). Although the only Archean rocks known in the block are the ~2.9 Ga Kongling Complex which was metamorphosed to granulites at 2.03–1.97 Ga and was intruded by ~1.85 Ga mafic dykes and A-type granites, a widespread Archean to Paleoproterozoic basement is inferred from detrital zircon U-Pb ages and Lu-Hf isotopic compositions (Gao et al., 2001; Zhang et al., 2006a, 2006b, 2011; Sun et al., 2008; Xiong et al., 2009; Peng et al., 2009). However, the Paleoproterozoic tectonic evolution of the Yangtze Block and its reconstruction in the Paleoproterozoic Columbia supercontinent are still poorly known. Recently, the Hekou, Dahongshan and Dongchuan Groups and some mafic plutons in the southwestern Yangtze Block have been dated at ~1700 Ma (Zhou, 2005; Greentree and Li, 2008; Zhao et al., 2010), but their implications for the reconstruction of the Yangtze Block in Columbia have not yet examined.

Sedimentary rocks are natural samples of eroded continental crust and may contain valuable information about their sources (Horton et al., 2010). Detrital zircon age spectra record various sources linked to eustatic, depositional and tectonic change (Wang et al., 2010, 2012a, 2012b), and thus can provide insights into the basin-orogen coupling and paleogeographic reconstructions (Horton et al., 2010; Myrow et al., 2010). On the other hand, mafic rocks directly derived from the mantle can be used for discriminating tectonic settings (Pearce and Cann, 1973). Therefore,

* Corresponding author. Tel.: +86 852 2857 8251.
E-mail address: mfzhou@hku.hk (M.-F. Zhou).

0301-9268/$ – see front matter © 2013 Elsevier B.V. All rights reserved.
http://dx.doi.org/10.1016/j.precamres.2013.03.011

studies combining sedimentary and interlayered mafic volcanic rocks can provide more reliable constraints tectonic environments and reconstruction of supercontinents in the earth's history.

In this contribution, we present new zircon U-Pb ages for metatuffs from the Hekou Group and for metagabbro from intruding mafic plutons, and detrital zircon ages of meta-siltstone. Whole-rock geochemistry and Nd-Hf isotopic compositions of mafic rocks are used to address their petrogenesis and tectonic settings. These new dataset are used to examine the Paleoproterozoic tectonic evolution of the western Yangtze Block, which is compared with other continents, and thus provide an excellent opportunity to explore the position of the Yangtze Block in Columbia.

2. Geological background

South China consists of the Yangtze Block in the northwest and the Cathaysia in the southeast. The Yangtze Block is bounded by the Songpan-Ganze Terrane of the Tibetan Plateau to the west and is separated from the North China Craton by the Qinlin-Dabie-Sulu Orogen to the north (Fig. 1). The southwestern Yangtze Block is marked by the Cenozoic Ailaoshan-Red River shear zone. Rare basement rocks are exposed in the Yangtze Block due to a thick Neoproterozoic (Sinian) to Cenozoic cover. The only known Archean rocks are the ~2.9 Ga Kongling Complex in the northern part of the block (Fig. 1) (Gao et al., 2001), consisting of tonalitic-trondhjemitic-granodioritic (TTG) gneisses, amphibolites, and meta-sedimentary rocks (Qiu et al., 2000). These Archean rocks were metamorphosed to granulites between 2.03 and 1.97 Ga (Qiu et al., 2000; Ling et al., 2001; Zhang et al., 2006b). The Kongling Complex was intruded by numerous ~1.85 Ga mafic dykes and granitic intrusions forming in a continental rift setting (Peng et al., 2009; Xiong et al., 2009; Zhang et al., 2011).

In the western Yangtze Block, late Paleoproterozoic to Neoproterozoic strata are widespread. Paleoproterozoic strata include the Dahongshan, Dongchuan and Hekou Groups, whereas Meso- to Neo-Proterozoic strata include the Kunyang, Huili, Julin and Yanbian Groups (Fig. 1). The Dahongshan and Dongchuan Groups contain tuffaceous layers with zircon U-Pb ages of ~1700 Ma (Hu et al., 1991; Greentree and Li, 2008; Zhao et al., 2010), whereas the Mesoproterozoic Kunyang and Huili Groups contain volcanic layers with zircon U-Pb ages of ~1100 to ~1000 Ma (Greentree et al., 2006; Geng et al., 2007; Sun et al., 2009). The Neoproterozoic Yanbian Group has detrital zircons as young as ~860 Ma (Zhou et al., 2006; Sun et al., 2009). The Paleoproterozoic Dahongshan, Dongchuan and Hekou Groups were metamorphosed to upper greenschist-lower amphibolite facies (Li et al., 1988), and were intruded by Paleoproterozoic gabbroic plutons (Zhao et al., 2010; Guan et al., 2011; Zhao and Zhou, 2011). In contrast, the Kunyang, Huili and Yanbian Groups underwent only lower greenschist facies metamorphism (Chen and Chen, 1987; Li et al., 1988).

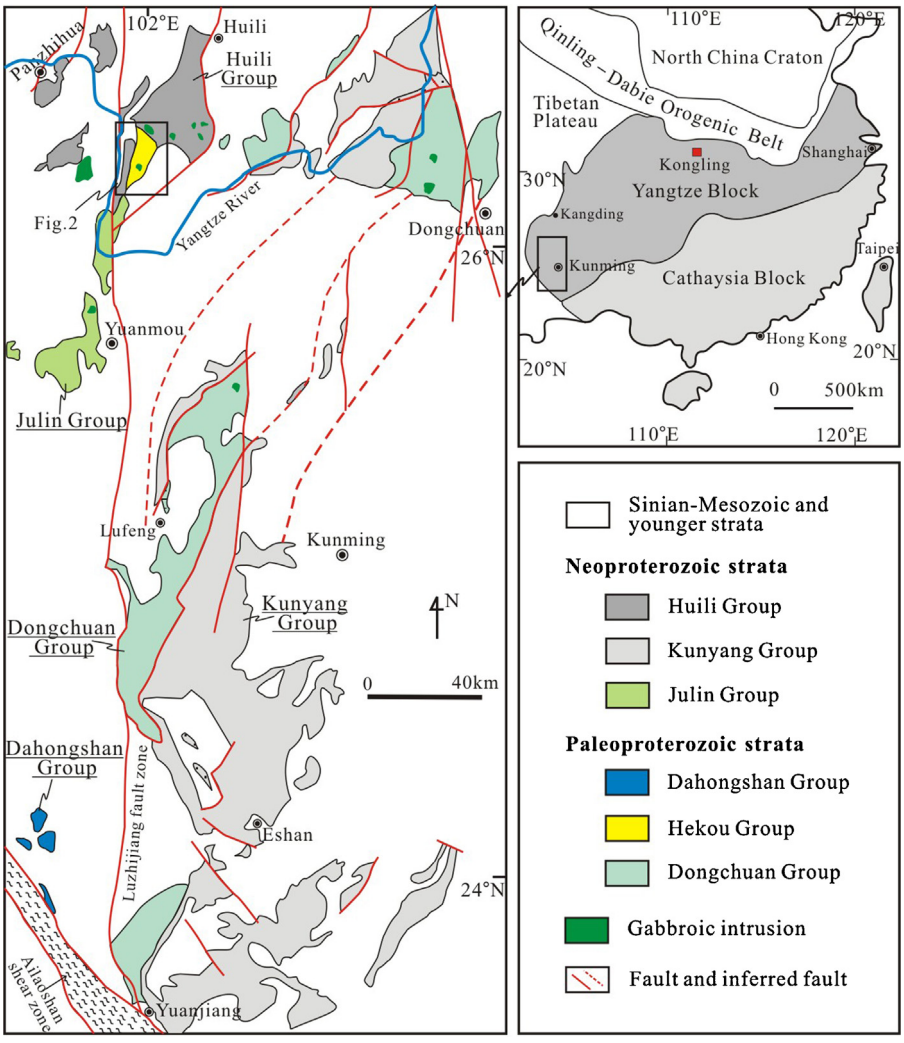

Fig. 1. Regional geological map of the western Yangtze Block showing the distribution of Precambrian strata and plutons (modified after Wu et al., 1990; Zhao et al., 2010).

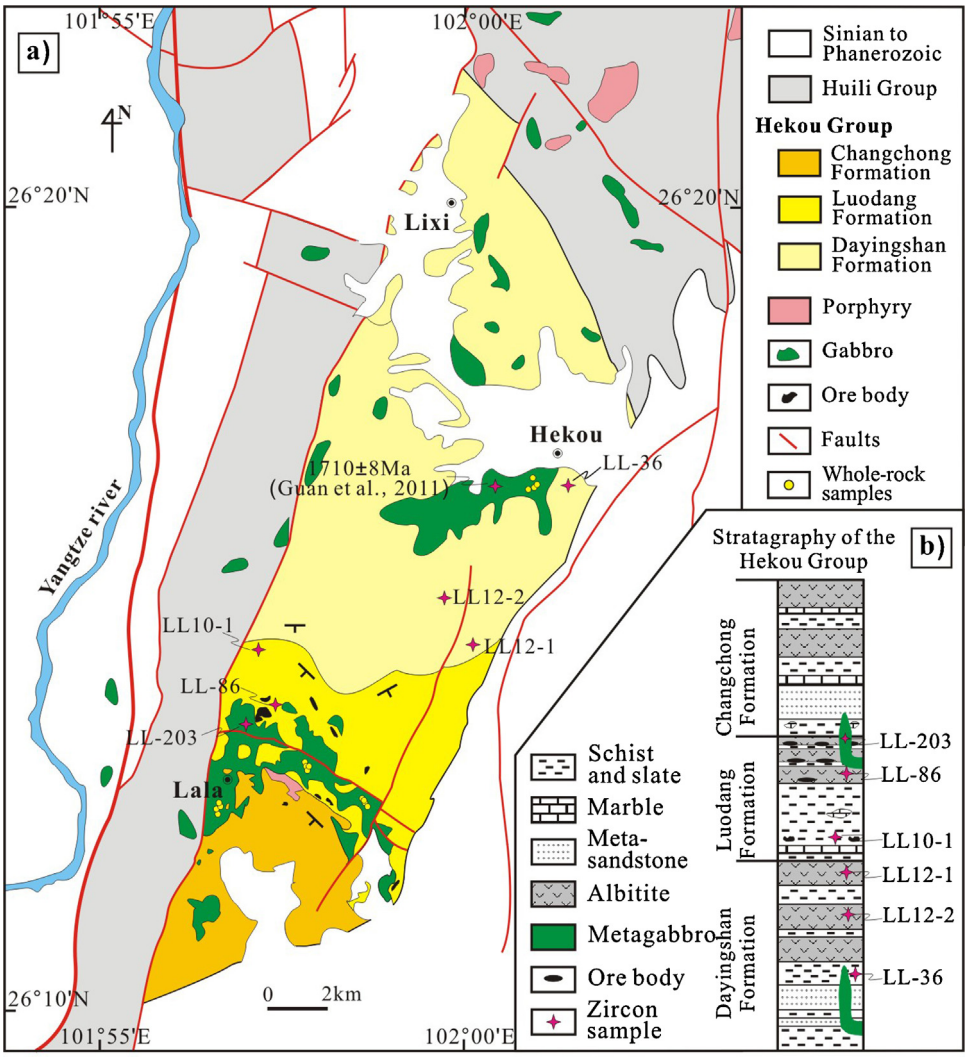

Fig. 2. (a) A simplified geological map of the Hekou area (after SBGMR, 1991). (b) A simplified stratigraphic column of the Hekou Group. Also shown are locations of samples for zircon U-Pb dating and whole-rock geochemical analyses.

Intruding the Meso- to Neo-Proterozoic strata in the region, numerous Neoproterozoic igneous rocks including granites, diorites and gabbros have ages ranging from ~860 to ~740 Ma (Zhou et al., 2002a, 2002b, 2006; Li et al., 2003; Zhao et al., 2008a, 2008b). Genesis of these rocks is still a matter of debate, but they have been interpreted to be either arc-related (Zhou et al., 2002a, 2002b, 2006; Zhao and Zhou, 2007) or mantle plume-related (Li et al., 2003).

3. Field relations

The Hekou Group covers a triangular area of approximately 35 km^2 in the Hekou area, Huili County in southwestern Sichuan Province. It is intruded by numerous mafic plutons, lamprophyre, and felsic dykes (Fig. 2). The Hekou Group hosts abundant Fe-Cu ore bodies in the Lala mine, which are generally stratabound, hosted in albitites and schists, and accompanied by extensive albitization, magnetite alteration and carbonatization (Chen and Zhou, 2012).

3.1. Hekou Group

The Hekou Group is in fault contact with the Huili Group to the west and northeast, and is unconformably overlain by Sinian and younger strata to the northwest and east/southeast (Fig. 2a). The strata locally show strong schistosity and are tightly foliated and/or folded. The schistosity is roughly SE-NW-striking and SW-dipping (Li et al., 1988; Ran et al., 1994). Sedimentary structures such as cross-bedding are locally preserved (He et al., 2010).

The Hekou Group has a total thickness of >1800 m, and comprises the Dayingshan, Luodang and Changchong Formations from the base upward (cf. Zhou, 2005). Each formation is generally composed of lower meta-sedimentary and upper meta-volcanic rocks (Fig. 2b) (SBGMR, 1991). Sedimentary rocks have rhythmical sequences of magnetite-bearing quartzite, meta-siltstone, slate, schist and phyllite (Fig. 3b) locally covered by siderite, marble or dolomite marble (Li et al., 1988). Volcanic rocks are dominantly felsic and mostly have been extensively altered to albitites (SBGMR, 1991), and subordinate interbeded meta-tuffs and metabasalts (Fig. 3d). The metabasaltic interlayers are generally 0.5–1 m thick (Fig. 3c). Some of albitites and meta-tuffs have pseudomorphic porphyric structures with feldspar phenocrysts.

3.2. Mafic plutons

Several mafic plutons intrude the Dayingshan and Luodang Formations along roughly NW-striking regional faults (Guan et al., 2011). Some occur as sills along lithologic contacts (Fig. 3d), which were previously thought to be sub-volcanic rocks of the Hekou Group (SBGMR, 1991). These mafic plutons are primarily composed

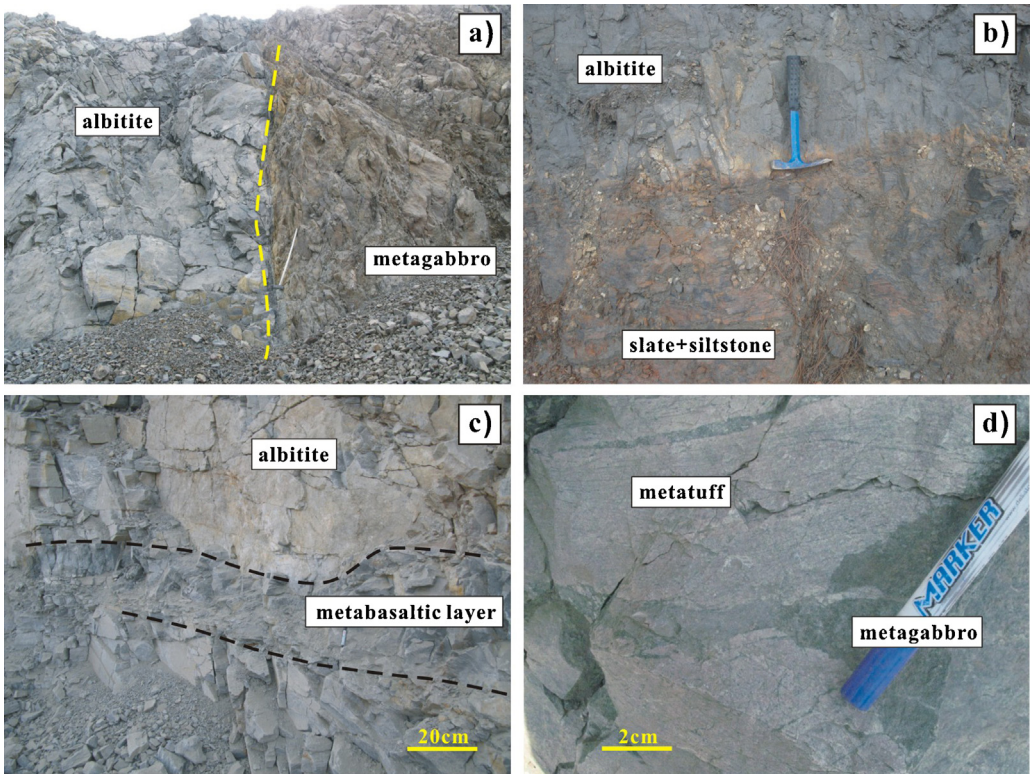

Fig. 3. Field photos of the Hekou Group and mafic plutons. (a) Metagabbro intrudes albitites of the Hekou Group. (b) Interbeds of black slate, metasiltstone and albitite in the Luodang Formation. (c) Metabasaltic layer within massive albitites of the Luodang Formation. (d) Reddish-pink metatuff in the Luodang Formation, which is intruded by metagabbro.

of gabbros which have undergone upper greenschist-lower amphibolite facies metamorphism. They display well developed foliations similar to the strata of the Hekou Group (Fig. 3a). In the Lala mine, mafic rocks close to ore bodies are commonly crosscut by numerous calcite-quartz-chalcopyrite veinlets, which are accompanied by alterations of chlorite, actinolite, albite and magnetite (Chen and Zhou, 2012).

4. Samples and analytical methods

In order to reduce the possible alteration effects, all samples were collected away from ore bodies. Sedimentary rocks used for separating detrital zircon grains are meta-siltstones which are composed of fine-grained sericite, quartz and feldspar (Fig. 4b). Metatuffs for zircon separation are reddish-pink (Fig. 3d), and have relic porphyritic texture with albite or K-feldspar phenocrysts in a matrix composed of albite, quartz, sericite and Fe-oxides (Fig. 4c). Locations of samples for zircon dating are indicated in Fig. 2. Meta-volcanic rocks for whole-rock geochemical analyses are amphibolites and chlorite-amphibole schists collected from the Dayingshan and Luodang Formations. They occur as interlayers among meta-sedimentary rocks, tuffs and albitite (e.g., Fig. 3c). They are composed chiefly of albite (40–50 vol.%), amphibole (40–60 vol.%), chlorite (<20 vol.%) and minor biotite (<10 vol.%) (Fig. 4a), and are considered to be basaltic (Xiao and Sun, 1992). Metagrabbroic rocks used for whole-rock geochemical analyses are from two gabbroic intrusions near Lala and Hekou Towns (e.g., Fig. 2a). Metagabbroic rocks from both intrusions are composed of variable amounts of plagioclase, clinopyroxene, albite and amphibole with minor magnetite, biotite, and chlorite (Fig. 4d). Gabbroic texture and minor clinopyroxene and plagioclase (An = ~55; Zhou, 2005) are locally preserved.

4.1. LA–ICP–MS zircon U-Pb dating

Zircon grains were separated using magnetic and heavy liquid techniques, mounted in epoxy and polished to about half their thickness. Cathodoluminescence imaging (CL) was used to investigate crystal morphologies and internal structure and to select analytical spots. Zircon grains were analyzed for U-Pb isotopes using the Nu Instrument multi-collector inductively coupled plasma–mass spectrometry (MC–ICP–MS), attached to the Resonetics RESOlution M-50-HR Excimer Laser Ablation System, at the University of Hong Kong. Analyses were performed with a beam diameter of 30 μm, 6 Hz repetition rate. Data acquisition started with a 30 s measurement of gas blank during the laser warm-up time. Typical ablation time was 40 s for each measurement, resulting in pits of 30–40 μm depth. ^{232}Th, ^{208}Pb, ^{207}Pb, ^{206}Pb, ^{204}Pb were simultaneously measured in static-collection mode. External corrections were applied to all unknowns, and standard zircons 91,500 and GJ were used as external standards and were analyzed twice before and after every 10 analyses. The raw data were reduced firstly by ICPMSDataCal program (Liu et al., 2008) and then were processed using the ISOPLOT program (Ludwig, 2003). Uncertainties in Appendix I are reported at the 1σ level.

4.2. Whole-rock major and trace elemental analyses

Samples were crushed and powered to at least 200 meshes in an agate mill. Whole-rock major and trace elemental analyses were conducted at the Guangzhou Institute of Geochemistry, Chinese Academy of Sciences, Guangzhou, China. Major elements were determined by X-ray fluorescence spectrometry (XRFS) using fused glass beads with analytical uncertainties between 1% and 5%. Trace elements were determined by a Perkin-Elmer Sciex ELAN 6000 ICP–MS, following the procedures described in Li et al. (2006). The

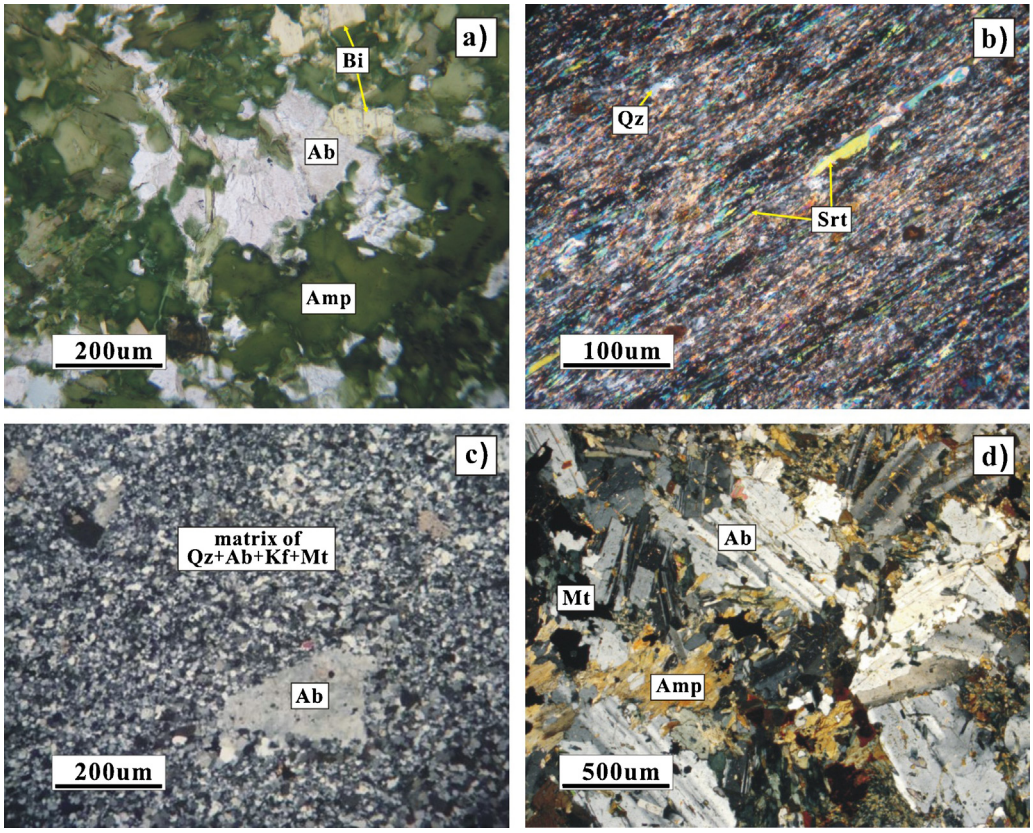

Fig. 4. Photomicrographs of different rocks. (a) Metabasalt consists chiefly of biotite, albite and amphibole. Cross-polarized light; (b) Foliated metasiltstone consists of quartz, sericite and albite with minor magnetite. Cross-polarized light; (c) Metatuff has a relic phenocryst of potassic-feldspar, and the matrix consists of quartz, albite, K-feldspar and magnetite. Cross-polarized light; and (d) Metagabbro is dominated by albite and amphibole with relic gabbroic texture. Cross-polarized light. Mineral abbreviations: Mt-magnetite; Kf-potassic feldspar; Bi-biotite; Ab-albite; Qz-quartz; Amp-amphibole; Srt-sericite.

USGS standard, BHVO-2 (Hawaii basalt) and Chinese national standards, AGV-1 (andesite) and GSR-3 (basalt), were used as reference materials. The accuracies of the ICP–MS analyses are better than ±5% (relative) for most elements.

4.3. Whole-rock Sm-Nd isotope analyses

Sample powders were dissolved in Teflon bombs with $HF + HNO_3$ acid, and separated by the conventional cation-exchange technique. The Nd isotopic measurements were conducted on a Thermo TRITON TI Thermal Ionization Mass Spectrometry (TIMS) at the Institute of Geochemistry, Chinese Academy of Sciences, Guiyang. The mass fractionation correction for Nd isotopic ratios was based on $^{146}Nd/^{144}Nd = 0.7216$. The USGS standard, BCR-2 (basalt), measured together with samples, has an average $^{146}Nd/^{144}Nd$ ratio of 0.512624 ± 0.000002.

4.4. Zircon Lu-Hf isotope analyses

Zircon Lu-Hf isotopes of the dated zircon grains were analyzed using a Geolas 193 nm excimer ArF laser-ablation system, attached to a Nu Plasma MC ICP–MS, at Northwest University, Xi'an, China. The analytical protocol used was similar to that outlined in Yuan et al. (2008). A stationary spot was used with a beam diameter of ~40 μm, an 8 Hz repetition rate and a laser power of 100 mJ/pulse. Zircon 91,500, GJ-1 and Monastery were used as reference standards. The measured $^{176}Lu/^{177}Hf$ ratios and the ^{176}Lu decay constant of 1.867×10^{-11} year^{-1} reported by Söderlund et al. (2004) were used to calculate initial $^{176}Hf/^{177}Hf$ ratios. The chondritic values of $^{176}Hf/^{177}Hf$ and $^{176}Lu/^{177}Hf$ reported by Blichert-Toft and Albarede (1997) were used for calculating $\varepsilon Hf(t)$ values. Single-stage model ages (T_{DM1}) were calculated using the present-day ratios of $^{176}Hf/^{177}Hf$ (0.28325) and $^{176}Lu/^{177}Hf$ (0.0384) (Griffin et al., 2000). Two-stage model ages (T_{DM2}) were calculated by projecting the initial $^{176}Hf/^{177}Hf$ ratios of the zircon back to the depleted mantle model growth curve, assuming a $^{176}Lu/^{177}Hf$ value of 0.022 for the average continental crust (Amelin et al., 1999).

5. Results

5.1. Zircon U-Pb ages of metatuffs

Zircon separates from three metatuffs were analyzed. Samples, LL12-1 and LL12-2, were collected from the upper and middle Dayingshan Formation, respectively. Sample LL-86 was collected from the Luodang Formation near the Lala mine (Fig. 2). Zircon grains from these samples are pinkish in color and show regular oscillatory zoning in the CL images (Fig. 5).

Thirty zircon grains from sample LL12-1 have narrow ranges of U (40–60 ppm) and Th (30–55 ppm) with Th/U ratios varying from 0.4 to 1.4 (Appendix I). Most grains have nearly concordant U-Pb ages, except one grain (spot 10) with obvious discordance (Fig. 5). All analyses of this sample yield an upper intercepted age of 1705 ± 6 Ma (MSWD = 0.99; Fig. 5), similar to the mean $^{207}Pb/^{206}Pb$ age of 1703 ± 5 Ma for the concordant analyses within uncertainty.

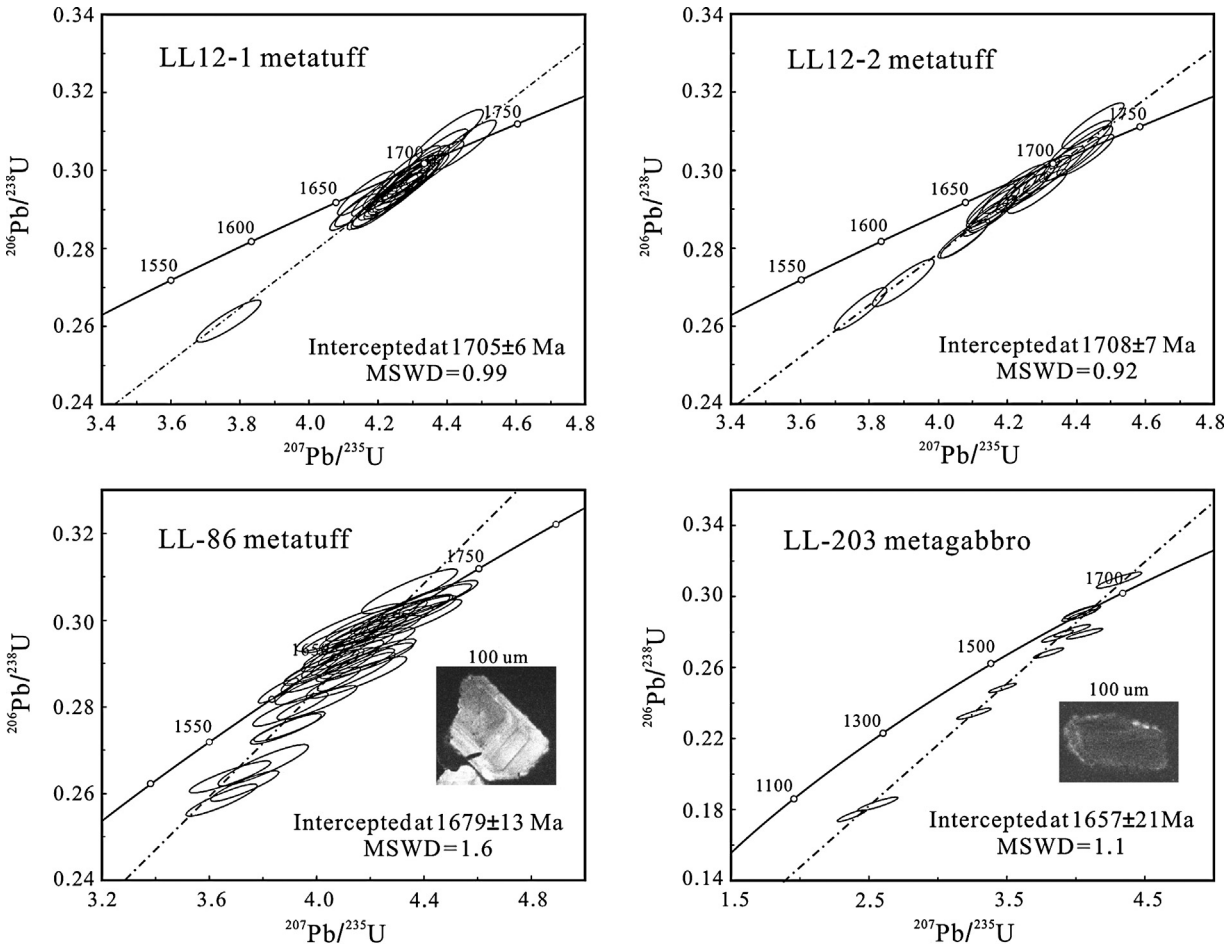

Fig. 5. U-Pb isotopic concordia plots of zircon grains from three metatuff and one metagabbro samples.

Twenty-eight zircon grains from sample LL12-2 have low to moderate U (35–122 ppm) and Th (10–89 ppm) with Th/U ratios mostly ranging from 0.5 to 1.5 (Appendix I). Two analyses (spots 12 and 19) were excluded from age calculations as they were determined to be xenocrystic due to much older apparent ages (Appendix I). Analyses of spots 17 and 28 were also excluded because of their large discordances (Appendix I). The remaining 24 analyses yield an upper intercepted age of 1708 ± 7 Ma (MSWD = 0.92; Fig. 5), similar to that of sample LL12-1 within uncertainty.

Forty-four zircon grains from sample LL-86 have generally high Th/U ratios (mostly >0.6; Appendix I). Less than half of the analyses have disconcordant ages (Fig. 5) because of lead loss. However, they have a narrow range of $^{207}Pb/^{206}Pb$ ages and all spots plot at a lead loss line, except for spots 17 and 38 which have relatively young $^{207}Pb/^{206}Pb$ ages probably due to younger metamorphism or alteration. The remaining 42 analyses yield an upper intercepted age of 1679 ± 13 Ma (MSWD = 1.6; Fig. 5).

5.2. Zircon U-Pb age of mafic pluton

A metagabbro sample, LL-203, was collected from a mafic pluton intruding the Luodang Formation near the Lala mine. Twelve zircon grains from this sample are prismatic and subhedral with lengths mostly smaller than 80 μm. Most grains have weak oscillatory zoning (Fig. 5), but have high Th/U ratios (>0.6; Appendix I), indicative of a magmatic origin. Only three grains have concordant ages, but the remaining 9 analyses have similar $^{207}Pb/^{206}Pb$ ages and plot in a discordia line. These 12 analyses yield an upper intercepted age of 1657 ± 21 Ma (MSWD = 1.1), interpreted to be the crystallization age of the mafic pluton.

5.3. Detrital zircon U-Pb ages

More than 140 detrital zircon grains from two meta-siltstone samples from the Hekou Group were determined for U-Pb ages (Appendix II). Sample LL-36 was collected from the Dayingshan Formation, and sample LL10-1 was collected from the lower Luodang Formation (Fig. 2). Analyses of zircon grains from both samples show a large discordant population with less than half of analyses having >90% concordance (Fig. 6).

Most zircon grains from sample LL10-1 have $^{207}Pb/^{206}Pb$ ages with two clusters at around 1950–1700 Ma and 2360–2160 Ma. Grains of these two clusters form two discordant lines with upper intercept ages of 1917 ± 32 and 2333 ± 32 Ma, respectively (Fig. 6a and b). The remaining grains have concordant or nearly concordant ages at 2900–2700 Ma. Two concordant grains (spots 10 and 67; Appendix II) have a mean $^{207}Pb/^{206}Pb$ age of 1768 ± 25 Ma. Eight youngest grains with concordant ages have a mean $^{207}Pb/^{206}Pb$ age of 1703 ± 5 Ma (Fig. 6b), similar to that of the tuff sample LL12-1.

In sample LL-36, zircon grains with ages older than 2000 Ma have $^{207}Pb/^{206}Pb$ ages with two clusters forming two discordia lines which give upper intercept ages of 2071 ± 10 and 2259 ± 19 Ma (Fig. 6c). In contrast, younger grains with $^{207}Pb/^{206}Pb$ ages <2000 Ma generally form four groups. Two younger groups

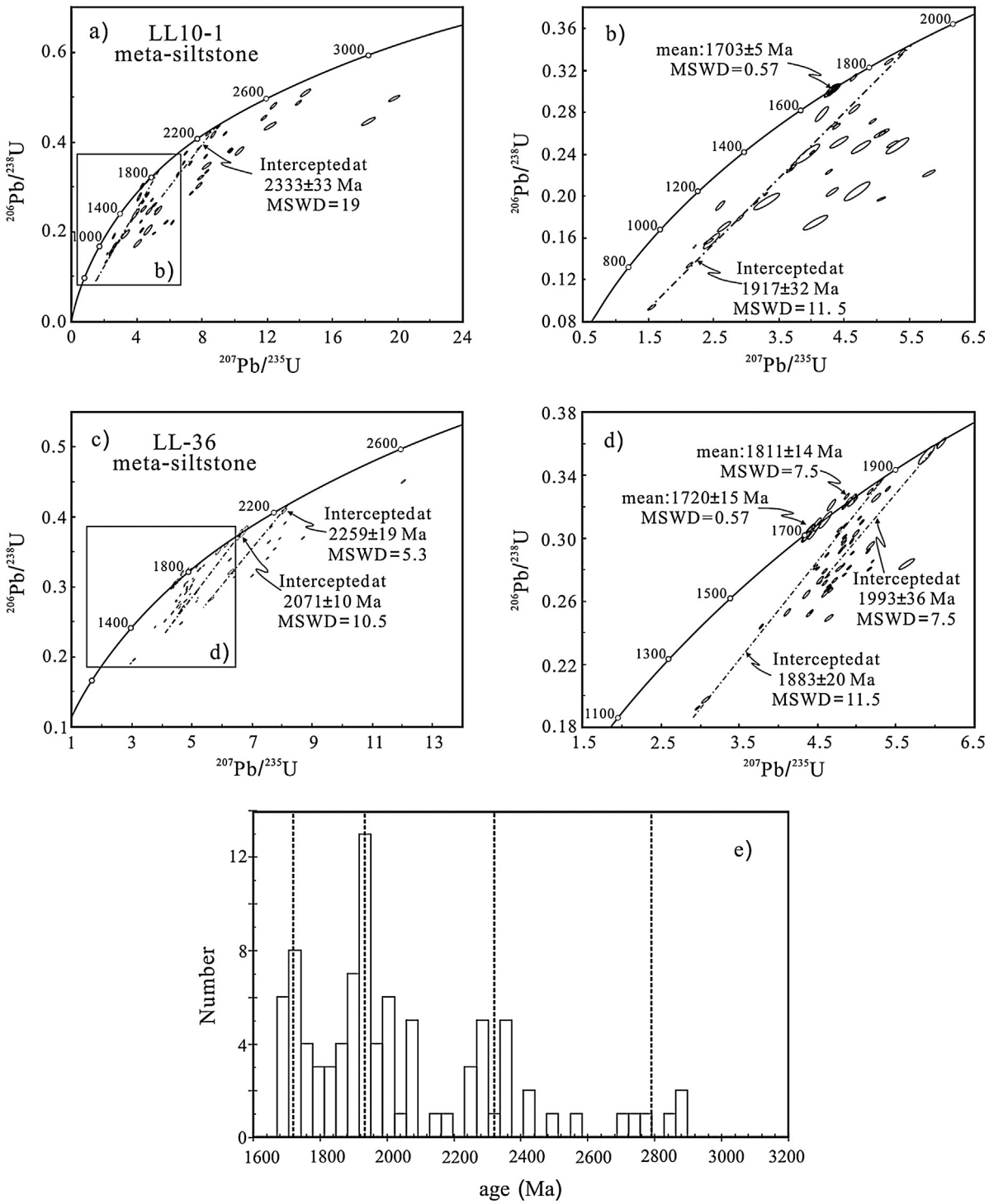

Fig. 6. U-Pb isotopic concordia plots and age histograms of detrital zircon grains from two meta-siltstone samples of the Hekou Group.

have concordant ages with mean $^{207}Pb/^{206}Pb$ ages of 1720 ± 15 and 1811 ± 14 Ma, respectively (Fig. 6d). In contrast, zircon grains of the two older groups generally have discordant ages, which form two discordant lines with upper intercept ages of 1883 ± 20 and 1993 ± 36 Ma (Fig. 6d).

Moreover, using the zircon grains with concordance >90%, we obtain a probability density histogram showing that detrital zircon grains from the two meta-siltstone samples have four major age populations at 1810–1770, 2070–1880, 2360–2160 and 2900–2700 Ma (Fig. 6e).

6. Whole-rock geochemistrical compositions

6.1. Major and trace elemental compositions

Although the least altered rocks are selected, most analyzed samples still have high LOI (loss on ignition) up to 9.32 wt.% (Table 1). In such a case, major elements have been normalized to 100 wt.% on a volatile free basis (Table 1). On the Zr/TiO_2 versus Nb/Y diagram of Pearce (1996), both metabasalts and metagabbros plot into the subalkaline and alkaline basalt fields (Fig. 7).

Table 1
Major and trace elemental compositions of the metabasalts and metagabbros in Hekou.

Rock	Metabasalts							Metagabbros			
Sample	ZK-4	ZK-81	ZK-89	ZK-91	ZK-117	ZK-119	ZK-121	LL-149	LL-154	LL-155	LL-164
SiO_2	48.03	44.82	52.24	51.88	52.18	47.71	48.74	47.86	47.97	47.97	46.18
TiO_2	2.32	1.67	2.61	2.45	1.86	2.28	2.66	3.75	4.77	3.55	4.74
Al_2O_3	13.88	15.94	10.34	13.39	13.91	15.39	13.28	13.33	11.60	10.03	15.54
Fe_2O_{3T}	21.21	19.22	14.79	18.51	14.96	16.08	18.33	14.29	13.02	12.22	16.71
MnO	0.20	0.37	0.18	0.10	0.09	0.13	0.20	0.20	0.27	0.39	0.24
MgO	1.69	2.81	10.09	2.10	5.13	6.01	4.66	5.95	6.38	9.15	5.18
CaO	4.15	5.62	5.73	4.67	4.04	5.27	5.92	8.46	10.44	12.42	5.18
Na_2O	6.69	0.42	1.92	4.68	5.68	4.28	5.02	2.42	2.12	1.69	4.76
K_2O	0.94	8.45	1.77	1.75	2.02	2.55	1.01	3.28	3.02	2.23	0.57
P_2O_5	0.90	0.67	0.34	0.47	0.14	0.30	0.17	0.46	0.41	0.35	0.91
Total	100.00	100.00	100.00	100.00	100.00	100.00	100.00	100.00	100.00	100.00	100.00
LOI	2.84	6.00	4.28	2.17	0.23	2.92	1.29	8.59	7.36	9.32	5.17
V	193	122	327	343	303	285	433	320	348	304	209
Cr	30.0	40.0	760	100	150	132	57.5	46.8	251	447	0.87
Ni	23.0	21.0	142	47.0	52.0	49.1	52.9	32.7	70.9	128	8.60
Rb	24.9	168	64.5	62.8	101	68.6	13.7	69.5	69.7	47.5	16.9
Sr	149	93.3	241	115	36.9	85.7	41.3	273	322	259	156
Y	62.5	52.7	21.5	50.1	15.7	27.4	23.5	29.5	25.0	22.5	36.3
Zr	497	368	313	247	111	173	134	348	357	302	326
Nb	91.8	56.3	29.9	36.6	14.5	33.2	11.0	40.9	6.49	24.7	35.4
Cs	0.10	0.39	4.40	0.60	0.97	0.85	0.17	2.02	1.17	1.04	0.73
Ba	95.3	1465	437	114	82.9	958	186	595	647	664	132
La	108	40.0	41.9	39.0	17.9	29.7	6.30	62.6	48.1	40.3	35.6
Ce	189	68.7	89.7	84.3	36.8	59.8	15.2	127	104	90.0	81.5
Pr	21.1	7.92	11.1	11.0	4.44	7.70	2.39	16.4	14.4	12.3	11.3
Nd	81.6	31.3	43.2	45.5	16.1	28.9	10.7	59.9	53.9	47.1	43.7
Sm	15.9	8.50	8.08	10.9	3.16	5.87	3.14	10.5	10.4	9.34	8.89
Eu	8.27	10.9	2.49	5.97	0.83	2.90	1.07	3.05	2.93	2.63	2.83
Gd	15.7	11.3	7.11	10.5	2.97	5.99	3.73	8.89	8.72	7.92	8.31
Tb	2.43	1.82	0.95	1.74	0.44	0.97	0.69	1.23	1.17	1.08	1.26
Dy	13.5	10.3	4.54	9.47	2.41	5.67	4.39	6.16	5.86	5.23	6.90
Ho	2.65	2.15	0.84	1.84	0.52	1.10	0.90	1.13	1.00	0.90	1.40
Er	7.13	5.72	2.33	5.05	1.62	2.94	2.47	2.91	2.49	2.19	3.83
Tm	0.97	0.78	0.29	0.67	0.26	0.41	0.37	0.39	0.31	0.29	0.55
Yb	5.25	5.22	1.73	3.58	1.60	2.56	2.34	2.40	1.91	1.73	3.45
Lu	0.67	0.85	0.23	0.48	0.25	0.39	0.34	0.35	0.28	0.26	0.56
Hf	11.8	8.70	7.60	5.80	2.90	3.83	3.34	7.83	8.41	7.21	7.53
Ta	4.90	3.40	2.10	2.50	0.60	2.05	0.68	2.02	0.48	1.70	2.07
Th	8.41	2.18	5.87	3.03	2.13	2.64	1.12	7.61	5.44	4.72	2.98
U	9.33	9.96	1.21	1.78	0.76	5.27	4.62	4.76	3.73	3.45	7.50

Rock	Metagabbros										
No.	LL-166	LL-168	LL-169	LL-170	LL-179	LL-180	LL-182	LL-198	LL-200	LL-203	LL-207
SiO_2	48.02	52.94	49.67	45.74	47.39	46.96	46.41	47.79	49.76	48.94	47.00
TiO_2	4.20	2.74	3.80	3.71	2.69	3.19	2.66	2.91	1.87	1.88	5.28
Al_2O_3	13.46	13.83	12.49	14.46	11.87	15.24	16.06	10.60	13.96	14.22	14.70
Fe_2O_{3T}	14.53	11.03	12.59	15.61	13.29	14.51	14.40	13.78	14.95	15.22	15.26
MnO	0.24	0.20	0.23	0.24	0.17	0.23	0.52	0.19	0.16	0.17	0.21
MgO	4.62	3.14	5.46	7.07	8.66	7.10	8.22	10.61	5.84	6.30	5.19
CaO	6.69	7.78	8.38	7.30	10.97	5.67	5.35	10.74	7.82	8.27	5.53
Na_2O	5.68	7.11	5.72	4.11	3.12	4.67	3.85	1.84	4.58	4.03	5.33
K_2O	0.97	0.21	0.23	1.31	1.54	1.93	2.13	1.25	0.95	0.81	0.71
P_2O_5	1.58	1.01	1.43	0.44	0.31	0.50	0.40	0.29	0.11	0.15	0.79
Total	100.00	100.00	100.00	100.00	100.00	100.00	100.00	100.00	100.00	100.00	100.00
LOI	0.92	4.58	2.89	0.93	4.36	1.23	1.47	3.76	1.61	1.47	3.04
V	166	108	188	332	341	259	275	361	324	314	192
Cr	2.70	2.55	1.54	94.1	332	105	174	627	118	134	13.5
Ni	8.67	11.2	10.2	96.3	122	89.1	121	197	63.0	69.1	7.87
Rb	42.4	4.59	2.71	56.2	32.6	86.2	75.2	22.2	13.6	18.0	24.2
Sr	53.09	50.7	53.7	93.7	380	62.8	106	389	80.8	197	106
Y	53.9	56.8	65.5	27.3	18.6	30.2	24.6	20.2	18.4	23.1	36.1
Zr	291	345	341	207	199	258	174	247	94.8	113	198
Nb	41.9	46.4	46.0	16.9	28.2	29.2	27.9	24.1	8.19	9.12	10.5
Cs	0.62	0.16	0.21	0.77	0.30	1.44	1.43	0.27	0.20	0.66	0.94
Ba	114	22.0	15.4	193	449	361	426	421	339	323	126
La	32.1	28.3	28.5	29.4	27.0	33.4	25.8	38.7	4.32	10.2	22.9
Ce	82.1	68.2	74.3	66.5	61.7	71.6	57.0	84.3	10.9	25.0	56.4
Pr	12.8	10.4	12.1	9.09	8.61	9.92	7.72	11.4	1.71	3.70	8.54
Nd	56.5	45.5	53.9	36.1	30.9	39.7	29.5	43.4	7.94	16.0	37.7
Sm	13.2	10.9	14.5	7.83	6.64	8.30	6.32	8.14	2.31	4.24	8.81
Eu	3.65	2.54	3.65	2.40	2.02	2.54	1.98	2.37	0.70	1.42	2.65
Gd	12.6	11.0	14.6	7.38	5.58	8.08	6.13	6.86	2.73	4.61	8.75

Table 1 (*Continued*).

Rock	Metagabbros										
No.	LL-166	LL-168	LL-169	LL-170	LL-179	LL-180	LL-182	LL-198	LL-200	LL-203	LL-207
Tb	1.98	1.76	2.38	1.10	0.80	1.22	0.93	0.92	0.54	0.79	1.39
Dy	10.8	10.4	13.0	5.81	4.16	6.42	5.05	4.50	3.34	4.68	7.55
Ho	2.12	2.11	2.54	1.12	0.72	1.17	0.97	0.80	0.71	0.91	1.48
Er	5.55	5.70	6.58	2.84	1.88	3.08	2.44	1.96	2.00	2.46	3.90
Tm	0.76	0.82	0.87	0.38	0.25	0.41	0.32	0.26	0.29	0.35	0.55
Yb	4.62	5.19	5.51	2.32	1.51	2.59	2.01	1.56	1.87	2.16	3.37
Lu	0.69	0.78	0.81	0.33	0.22	0.37	0.30	0.23	0.27	0.30	0.51
Hf	7.61	10.3	8.14	4.82	4.83	5.46	3.87	5.84	2.43	2.84	4.70
Ta	2.65	2.96	2.82	1.03	1.82	1.72	1.69	1.52	0.52	0.63	0.62
Th	2.87	3.99	3.09	2.19	3.74	2.51	1.53	4.37	1.05	1.13	1.85
U	9.26	10.5	11.0	4.51	2.95	4.96	3.99	3.05	3.70	4.11	6.88

Fe_2O_{3T}: Fe_2O_3 total.

Metabasalts of the Hekou Group have wide ranges of Na_2O from 0.42 to 5.68 wt.% and K_2O from 0.90 to 8.45 wt.%. These rocks have 42.2–52.5 wt.% SiO_2 and 4.04–5.92 wt.% CaO with a wide range of MgO from 2.10 to 10.1 wt.%, and Fe_2O_3t from 14.1 to 20.6 wt.%. TiO_2 has a narrow range from 1.67 to 2.66 wt.% (Table 1; Fig. 8a). Metabasalts display LREE-enriched chondrite-normalized REE patterns (La/Yb_{CN} = 5.50–17.4) (Fig. 9). They mostly have positive Eu anomalies with Eu/Eu^* ($=Eu/(Sm \times Gd)^{1/2}$) values up to 3.4. In the primitive-mantle normalized spider-gram, they display slightly positive to negative Nb-Ta and Zr-Hf anomalies with variable $(Ta/La)_{PM}$ (0.56–1.81) and $(Hf/Sm)_{PM}$ (0.77–1.53) ratios (Figs. 8b and 10). In addition, all metabasalts display strongly negative Sr anomalies (Fig. 10). There are positive correlations between $(Ta/La)_{PM}$ and $(Hf/Sm)_{PM}$, and between Cr and Ni (Fig. 8b and c).

Metagabbros contain variable Na_2O (1.69–7.11 wt.%) and K_2O (0.21–3.28 wt.%), similar to metabasalts, but have relatively uniform SiO_2 (45.7–52.9 wt.%), Al_2O_3 (10.0–16.1 wt.%) and Fe_2O_3t (11.0–16.7 wt.%) (Table 1). TiO_2 range largely from 1.87 to 5.28 wt.%. Metagabbros have LREE-enriched chondrite-normalized REE patterns (La/Yb_{CN} = 3.39–18.70), except for sample LL-200 with relatively low REE (La_{CN} = 18.2) and flat REE pattern (La/Yb_{CN} = 1.66) (Fig. 9). They generally show negative Eu anomalies with Eu/Eu^* values varying from 0.71 to 1.01. In the primitive mantle-normalized spider-gram, all samples have a fractionated pattern characterized by variable enrichments of incompatible trace elements (e.g. Nb, Ta, Zr, Hf and REE) with respect to the primitive mantle (Fig. 10). Most samples display mildly positive to strongly negative Nb-Ta anomalies (Ta/La_{PM} = 0.17–1.75) but weak Zr-Hf anomalies (Hf/Sm_{PM} = 0.77–1.37) (Figs. 8b and 10). Sample LL-200, with less LREE enrichment, displays slightly positive Nb-Ta and

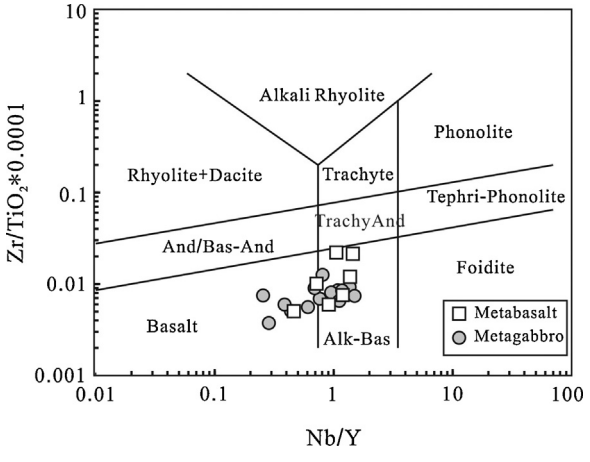

Fig. 7. Rock classification diagram of the metabasalts and metagabbros at Hekou (after Winchester and Floyd (1977), revised by Pearce, 1996).

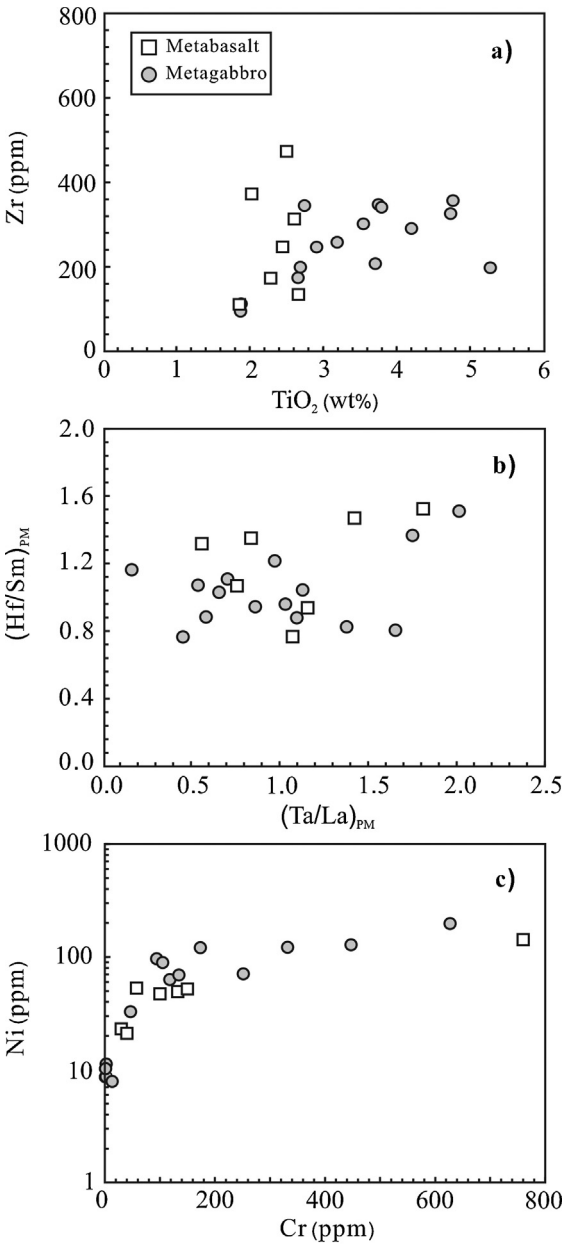

Fig. 8. Bi-elemental plots of the metabasalts and metagabbros at Hekou.

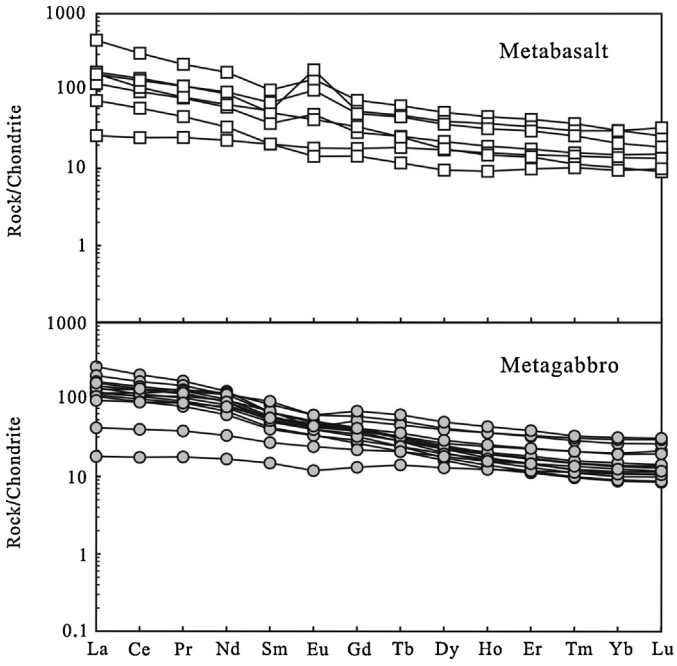

Fig. 9. Chondrite-normalized REE patterns of the metabasalts and metagabbros at Hekou. Chondrite values are after Sun and McDonough (1989).

Zr-Hf anomalies (Ta/La_{PM} = 2.02; Hf/Sm_{PM} = 1.51) (Fig. 10). All samples have negative Sr anomalies in the spider-gram, similar to metabasalts (Fig. 10).

6.2. Sm-Nd isotopes

Initial $^{143}Nd/^{144}Nd$ ratios of both metagabbros and metabasalts are calculated to $\varepsilon Nd(t)$ values using the age of 1700 Ma (Table 2). The calculated $\varepsilon Nd(t)$ values range from 0.2 to +3.4, and are below the depleted mantle line (Fig. 11a). The calculated depleted mantle model ages (T_{DM}) range from 2040 to 2900 Ma (Fig. 11a).

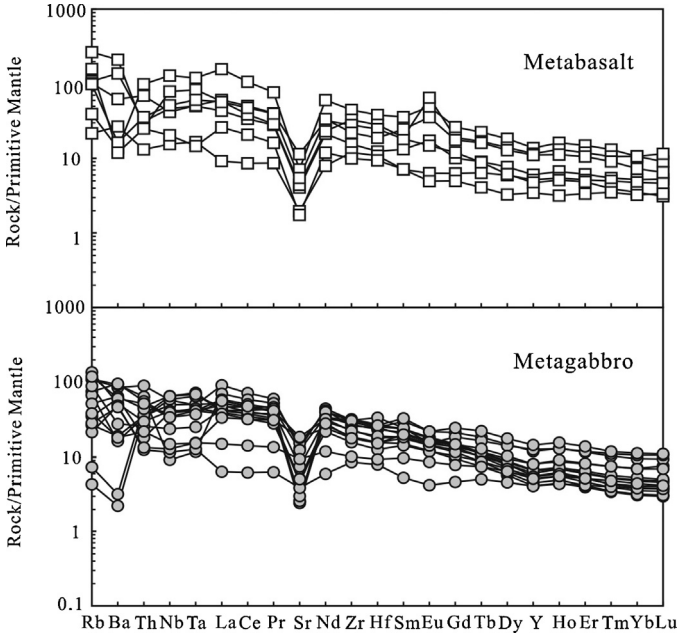

Fig. 10. Primitive-mantle normalized multi-elemental spider-grams of the metabasalts and metagabbros at Hekou. Primitive mantle values are after Sun and McDonough (1989).

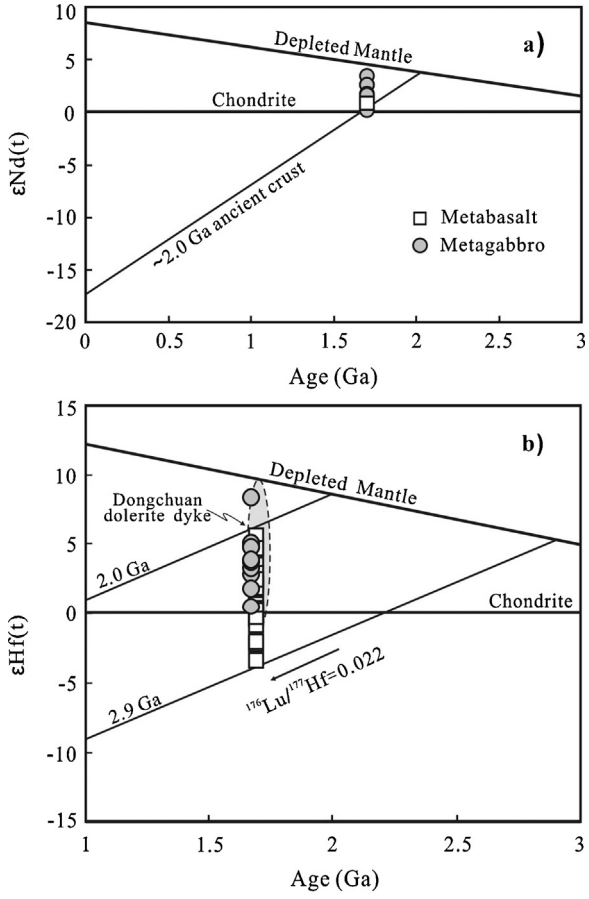

Fig. 11. (a) Plots of whole-rock $\varepsilon Nd(t)$ vs. age for the metabasalts and metagabbros at Hekou. (b) Plots of $\varepsilon Hf(t)$ vs. age for zircon grains from the metatuff and metagabbro at Hekou. The zircon $\varepsilon Hf(t)$ values of the Dongchuan dolerite dykes are from Zhao et al. (2010).

6.3. Zircon Lu-Hf isotopes

Lu-Hf analyses were conducted on dated zircon grains from both metatuff (LL-86) and metagabbro (LL-203). The initial $\varepsilon Hf(t)$ values of zircons and their depleted mantle model ages (T_{DM1} and T_{DM2}) were calculated using their crystallization ages (1680 Ma and 1660 Ma, respectively). These zircon grains from metatuff have variable $\varepsilon Hf(t)$ values from −3.3 to +5.7, slightly lower than those from metagabbro (+0.6 to +8.4) (Fig. 11b). They have one-stage Hf model ages of 1890–2240 Ma and 1770–2090 Ma (Table 3 and Fig. 11b), corresponding to two-stage Hf model ages of 2159–2956 Ma and 1902–2601 Ma, respectively (Table 3).

7. Discussion

7.1. Assessment of element mobility during metamorphism and alteration

Both basalts and gabbros from Hekou have undergone various degrees of metamorphism and alterations such as albitization and magnetite alteration, which may have caused large variations of LOI and major elements such as K_2O, Na_2O and Fe_2O_3t. However, the straight trends and clusters of generally immobile Ti, Zr, Hf, Nb, Ta, REE, Cr and Ni suggest that these elements were relatively immobile during hydrothermal alterations (e.g., Fig. 8), and thus can be used to examine the petrogenesis and tectonic environments of the mafic rocks.

Table 2
Whole-rock Sm-Nd isotopic compositions of the metabasalts and metagabbros in Hekou.

Sample	Rock	Age (Ma)	Sm (ppm)	Nd (ppm)	$^{147}Sm/^{144}Nd$	$^{143}Nd/^{144}Nd$	$\pm2\sigma$	$(^{143}Nd/^{144}Nd)_i$	$\varepsilon Nd(t)$	T_{DM} (Ma)
LL-166	Metagabbro	1700	13.2	56.5	0.1416	0.512145	02	0.510562	2.6	2117
LL-169	Metagabbro	1700	14.5	53.9	0.1628	0.512258	02	0.510438	0.2	2657
LL-170	Metagabbro	1700	7.83	36.1	0.1312	0.512032	03	0.510565	2.7	2058
LL-179	Metagabbro	1700	6.64	30.9	0.1299	0.512057	03	0.510604	3.4	1982
LL-180	Metagabbro	1700	8.30	39.7	0.1265	0.511979	02	0.510565	2.7	2040
LL-182	Metagabbro	1700	6.32	29.5	0.1295	0.511962	02	0.510514	1.7	2142
LL-200	Metagabbro	1700	2.31	7.94	0.1758	0.512473	02	0.510507	1.5	2710
LL-203	Metagabbro	1700	4.24	16.0	0.1606	0.512317	02	0.510521	1.8	2382
ZK-121	Metabasalt	1700	3.14	10.7	0.1769	0.512445	04	0.510467	0.8	2900

7.2. Petrogenesis of the mafic rocks

Both metabasalts and metagabbros have similar variations of chemical compositions and primitive mantle-normalized trace elemental patterns, suggesting that they are co-magmatic in origin. Although four metagabbric samples near Hekou town have higher TiO_2 than other metagabbros and metabasalts (Table 1), the linear correlations among different elements for all these samples suggest that such variations of TiO_2 are possibly due to fractional crystallization of ilmenite, titanite (Fig. 8a). Several samples of metabasalts have slightly positive Eu anomalies, possibly due to oxidized fluids-related alterations (Chen and Zhou, 2012). Low and variable Cr (mostly <200 ppm) and Ni (mostly <100 ppm) of these rocks, and a positive correlation between the two elements (Fig. 8c), possibly indicate fractional crystallization of mafic minerals such as olivine and pyroxenes.

In the primitive-mantle normalized spider-grams, some samples show variably negative Nb-Ta anomalies but slightly positive Zr-Hf anomalies (Fig. 10). These features can be potentially explained by crustal contamination, because continental crust is

Table 3
Zircon Lu-Hf isotopic compositions of the metatuff and metagabbros at Hekou.

Spot	Age (Ma)	$^{176}Yb/^{177}Hf$	$^{176}Lu/^{177}Hf$	$^{176}Hf/^{177}Hf$	1σ	Hf_i	$\varepsilon Hf(0)$	$\varepsilon Hf(t)$	T_{DM1} (Ma)	T_{DM2} (Ma)	$f_{Lu/Hf}$
LL-86: metatuff											
01	1680	0.026238	0.000971	0.281853	0.000035	0.281822	−32.5	3.8	1963	2327	−0.97
02	1680	0.044772	0.001598	0.281897	0.000029	0.281846	−30.9	4.7	1934	2249	−0.95
03	1680	0.028414	0.001037	0.281847	0.000026	0.281814	−32.7	3.6	1974	2349	−0.97
04	1680	0.040142	0.001438	0.281898	0.000029	0.281852	−30.9	4.9	1924	2230	−0.96
05	1680	0.052655	0.001849	0.281846	0.000026	0.281787	−32.8	2.6	2019	2436	−0.94
06	1680	0.020235	0.000727	0.281802	0.000024	0.281778	−34.3	2.3	2021	2463	−0.98
07	1680	0.024938	0.000943	0.281905	0.000026	0.281875	−30.7	5.7	1890	2159	−0.97
08	1680	0.066850	0.002363	0.281872	0.000034	0.281796	−31.8	2.9	2010	2406	−0.93
09	1680	0.027973	0.001023	0.281797	0.000028	0.281765	−34.5	1.8	2042	2506	−0.97
10	1680	0.023096	0.000858	0.281803	0.000027	0.281775	−34.3	2.2	2026	2472	−0.97
11	1680	0.043055	0.001569	0.281900	0.000026	0.281850	−30.9	4.8	1929	2238	−0.95
12	1680	0.024504	0.000922	0.281763	0.000027	0.281734	−35.7	0.7	2084	2603	−0.97
14	1680	0.031980	0.001166	0.281742	0.000031	0.281705	−36.4	−0.3	2127	2694	−0.96
15	1680	0.024538	0.000945	0.281809	0.000029	0.281779	−34.0	2.3	2021	2460	−0.97
16	1680	0.027122	0.000997	0.281687	0.000027	0.281655	−38.4	−2.1	2193	2850	−0.97
17	1680	0.027678	0.001012	0.281760	0.000026	0.281727	−35.8	0.5	2094	2623	−0.97
18	1680	0.026617	0.000962	0.281748	0.000031	0.281717	−36.2	0.1	2108	2656	−0.97
19	1680	0.031856	0.001135	0.281760	0.000030	0.281724	−35.8	0.3	2100	2634	−0.97
20	1680	0.054211	0.001898	0.281774	0.000028	0.281714	−35.3	0.0	2123	2666	−0.94
21	1680	0.026150	0.000967	0.281798	0.000028	0.281768	−34.4	1.9	2038	2497	−0.97
22	1680	0.042406	0.001535	0.281776	0.000027	0.281727	−35.2	0.4	2100	2625	−0.95
23	1680	0.040001	0.001437	0.281748	0.000033	0.281703	−36.2	−0.4	2133	2701	−0.96
24	1680	0.023842	0.000897	0.281686	0.000030	0.281658	−38.4	−2.0	2188	2841	−0.97
25	1680	0.028155	0.001042	0.281654	0.000027	0.281621	−39.5	−3.3	2240	2956	−0.97
26	1680	0.026858	0.000983	0.281740	0.000028	0.281709	−36.5	−0.2	2119	2682	−0.97
27	1680	0.030997	0.001155	0.281727	0.000024	0.281690	−37.0	−0.9	2147	2740	−0.97
28	1680	0.028835	0.001061	0.281753	0.000028	0.281720	−36.0	0.2	2105	2647	−0.97
29	1680	0.026645	0.000990	0.281738	0.000030	0.281706	−36.6	−0.3	2122	2689	−0.97
30	1680	0.036431	0.001321	0.281828	0.000030	0.281786	−33.4	2.5	2016	2439	−0.96
LL-203: metagabbro											
01	1660	0.047190	0.001762	0.281865	0.000030	0.281809	−32.1	2.9	1988	2392	−0.95
02	1660	0.063507	0.003374	0.282071	0.000029	0.281965	−24.8	8.4	1773	1902	−0.90
03	1660	0.079526	0.002814	0.281922	0.000028	0.281833	−30.1	3.8	1963	2317	−0.92
04	1660	0.081498	0.002970	0.281956	0.000032	0.281863	−28.9	4.8	1921	2225	−0.91
05	1660	0.085080	0.002696	0.281955	0.000030	0.281870	−28.9	5.1	1909	2202	−0.92
06	1660	0.099486	0.003047	0.281966	0.000033	0.281870	−28.5	5.1	1911	2201	−0.91
07	1660	0.118253	0.003237	0.281921	0.000034	0.281819	−30.1	3.3	1987	2360	−0.90
08	1660	0.041382	0.002279	0.281904	0.000028	0.281832	−30.7	3.7	1960	2320	−0.93
09	1660	0.042938	0.002264	0.281814	0.000026	0.281743	−33.9	0.6	2087	2601	−0.93
10	1660	0.077992	0.002386	0.281936	0.000036	0.281861	−29.6	4.8	1919	2229	−0.93
11	1660	0.067405	0.002360	0.281854	0.000027	0.281779	−32.5	1.9	2036	2487	−0.93
12	1660	0.072633	0.003086	0.281934	0.000028	0.281837	−29.6	3.9	1960	2305	−0.91

Hf_i: initial Hf isotopic compositions.

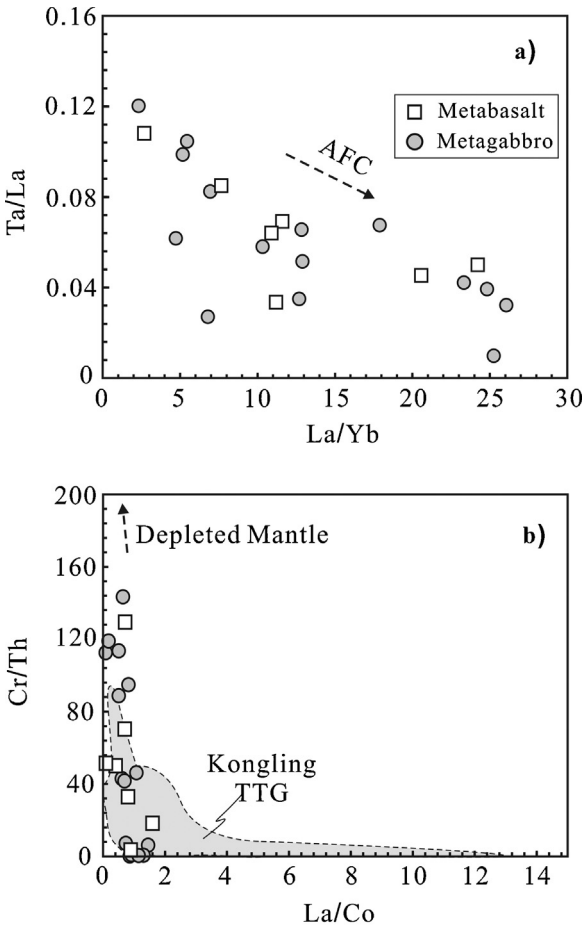

Fig. 12. Plots of Ta/La vs. La/Yb and Cr/Th vs. La/Co for the metabasalts and metagabbros in Hekou, showing a fractional crystallization and crustal assimilation (AFC) process.

poor in Nb-Ta but rich in Zr-Hf. Negative correlations of La/Yb versus Ta/La (Fig. 12a) and Cr/Th versus La/Co (Fig. 12b) are also consistent with an assimilation-fractional crystallization trend. In addition, these mafic rocks have variable εNd(t) and zircon εHf(t) values, and much older depleted mantle model ages (Tables 2 and 3), further indicating crustal contamination during magma ascending.

Some samples of both the metabasalts and metagabbros have positive εNd(t) (up to +3.1) and zircon εHf(t) (up to +8.4) values, and have relatively flat chondrite-normalized REE patterns (e.g., LL-200 and ZK-121) (Figs. 9 and 10), indicative of contributions from a depleted mantle source. Their magmatic zircons have Hf isotopic compositions similar to those of the ~1700 Ma dolerite dykes intruding the Dongchuan Group (εHf(t) = 0.3–10.4; Zhao et al., 2010) (Fig. 11b), which have been suggested to be derived from depleted mantle.

7.3. Intra-continental rifting environment

Volcanic rocks of the Hekou Group were previously thought to represent a spilite-keratophyre suite erupted in an ocean floor setting, based on solely the Na-rich features for the volcanic rocks (Xiao and Sun, 1992; Wu et al., 1998; Chen and Xia, 2001). Such high Na_2O and K_2O features are also considered to be typical of alkali basalts, but both elements are well documented to be mobile during regional albitization associated with the Fe-Cu mineralization at Lala (Chen and Zhou, 2012). In this consideration, we only use immobile trace elemental and Nd-Hf isotopic data to interpret that the co-magmatic Hekou metabasalts and metagabbros have formed in an intra-continental rift setting. Both metabasalts and metagabbros have trace elemental features similar to modern basalts in continental rifts (e.g. Rogers et al., 2000; Ritter et al., 2001), including enrichment of incompatible elements, such as TiO_2 (mostly >2.5 wt.%), Zr (94.8–497 ppm) and Th (1.05–7.61 ppm) (Table 3), right-sloping REE patterns (Fig. 8). Some samples with possibly least crustal contaminations (e.g., $Nb/La_{PN} > 1$) have high Nb/Y ratios (mostly >0.6) and weak anomalies of Nb-Ta and Zr-Hf (Fig. 10), further indicating a within-plate setting. Some triangular diagrams using immobile trace elements, such as Zr-Zr/Y, Zr-Ti-Y, Hf-Th-Ta and Zr-Nb-Y, are useful for tectonic discrimination of mafic rocks (Pearce and Cann, 1973; Pearce and Norry, 1979; Wood, 1980; Meschede, 1986). In these diagrams, samples without strong crustal contamination all plot in 'within-plate setting' fields (Fig. 13), further supporting a continental rift setting.

On the other hand, the intra-continental rift setting of the mafic rocks is also supported by locally unmodified sedimentary features and facies in the contemporaneous sedimentary rocks. For example, sandstone and siltstones are overlain by layers of carbonate and carbonaceous slate, which possibly indicates a lagoon or lacustrine environment. Such sedimentary features are similar to those of the contemporaneous Dongchuan and Dahongshan Groups which have been suggested to deposit in an intra-continental or aulacogen setting (Li et al., 1988; Wu et al., 1990; Xiao and Sun, 1992; He et al., 2010; Zhao et al., 2010). It is thus suggested that there would be a ~1.7 Ga SN-trend rift basin along a belt from Yuanjiang to Huili County in the western Yangtze Block (Fig. 1).

7.4. Provenance of sedimentary rocks from the Hekou Group

Detrital zircon grains from meta-siltstones of the Hekou Group have four major age populations at 1810–1770, 2070–1880, 2360–2160 and 2900–2700 Ma (Fig. 6e). The latter three age spectra are roughly similar to those of the coeval Dahongshan and Dongchuan Groups in this region (Greentree et al., 2006; Zhao et al., 2010; Wang et al., 2012a), suggesting that they may have similar provenances.

These Archean to Paleoproterozoic detrital zircon grains, can be broadly correlated with zircon ages of the magmatic and metamorphic rocks of the Yangtze Block (Greentree and Li, 2008; Zhao et al., 2010; Wang et al., 2012a). For example, 2900–2700 Ma population can be correlated with ~2900 Kongling Complex in the northern Yangtze Block; some 2070–1880 Ma detrital zircon grains with very low Th/U ratios (<0.1; e.g. spots 09, 11 and 20 of sample LL10-1) (Appendix II) may be metamorphic in origin, comparable to the 2050–1900 Ma Kongling and Huangtuling granulites (Gao et al., 2001; Ling et al., 2001; Zhang et al., 2006a). However, the 1810–1770 Ma and 2360–2160 Ma zircon populations are poorly documented and their source regions are not clear. As the two populations of detrital grains have not been previously recognized in the Yangtze Block, they may represent either an exotic or now totally concealed source region.

There are also some detrital zircon grains with ages (e.g., 1703 ± 5 and 1720 ± 15 Ma) similar or close to the deposition ages of the Hekou Group and mafic plutons, reflecting some of the sediments were possibly sourced from local coeval igneous rocks. This feature is different from that of the Dahongshan Group in which detrital zircon grains with ages close to the deposition age are largely absent (Greentree and Li, 2008). However, we cannot rule out the possibility that the two meta-siltstone samples from the

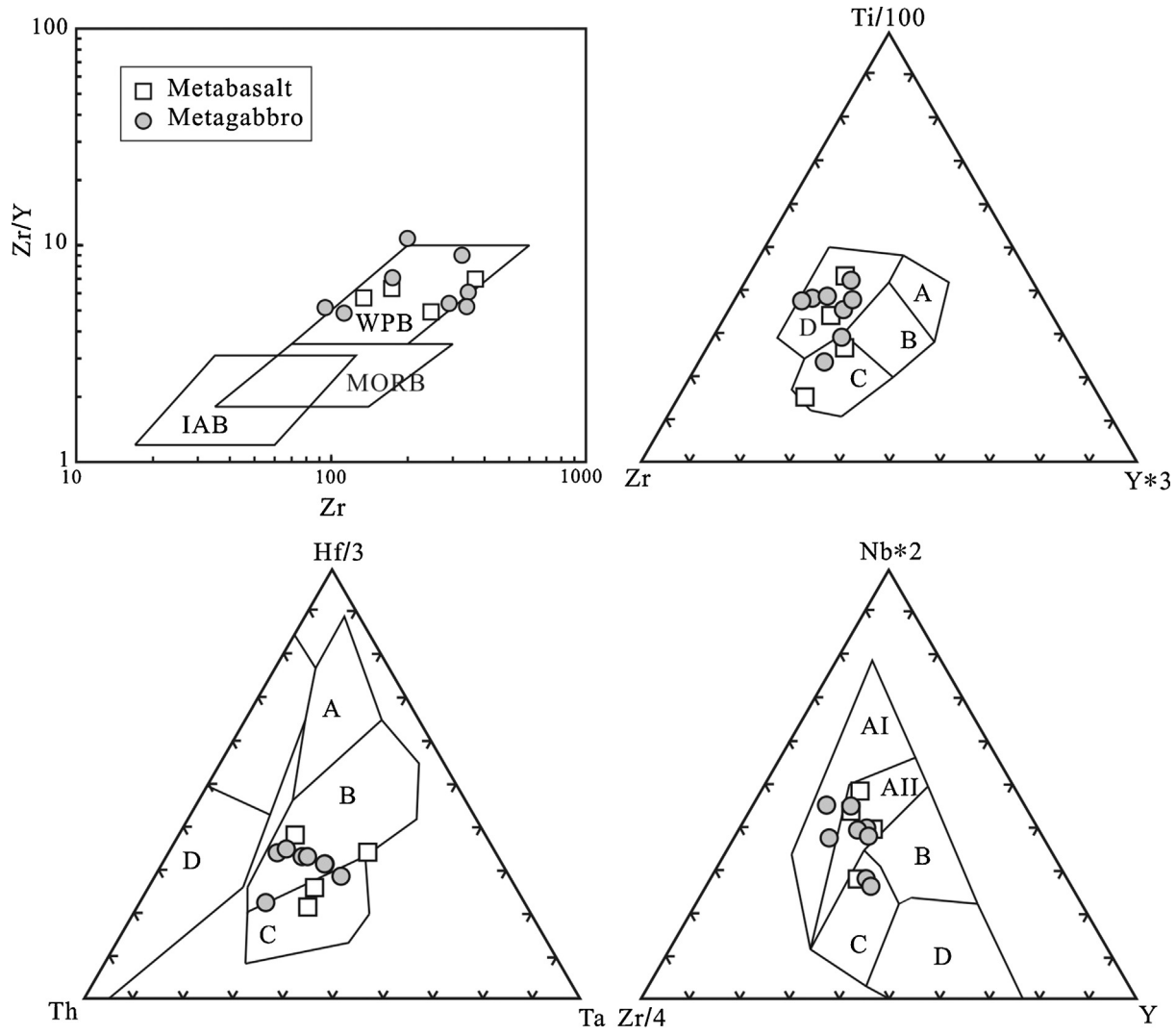

Fig. 13. Tectonic discrimination diagrams for the Hekou metabasalts and metagabbros. The Zr-Zr/Y diagram is after Pearce and Norry (1979); the Zr-Y*3-Ti/100 diagram is after Pearce and Cann (1973), and the fields are: A-island-arc tholeiites, B-MORB, island-arc tholeiites and calc-alkali basalts, C-calc-alkali basalts and D-within-plate basalts; the Th-Hf/3-Nb/16 diagram is after Wood (1980), and the fields are: A-N-type MORB, B-E-type MORB and within-plate tholeiites, C-alkaline within-plate basalts and D-volcanic-arc basalts; the Zr/4-Y-Nb*2 diagram is after Meschede (1986), and the fields are: AI-within-plate alkali basalts, AII-within-plate alkali basalts and tholeiites, B-E-type MORB, C-within-plate tholeiites and volcanic-arc basalts and D-N-type MORB and volcanic-arc basalts.

Hekou Group contain minor tuffaceous materials of ~1700 Ma, as their primary textures are modified by metamorphism.

7.5. Possible connection of the Yangtze Block with other cratons in Columbia

Global-scale 2.1–1.8 Ga collision and subsequent rifting events have been well documented in a number of large continental cratons, and are linked with the assemblage and break-up of the Columbia supercontinent (Rogers and Santosh, 2002; Zhao et al., 2002, 2004). The Yangtze Block has long been considered to be a younger continental fragment, and thus has not been placed in this Paleoproterozoic supercontinent. However, recently identified 2.05–1.90 Ga magmatism and granulite facies metamorphism in the northern Yangtze Block have been interpreted to be the evidence of the Yangtze Block involving in the assembly of Columbia (Zhang et al., 2006a, 2006b; Sun et al., 2008; Wu et al., 2008). Although no granulite facies rocks of Paleoproterozoic ages have been identified in the western Yangtze Block, the 2.05–1.95 Ga detrital zircons of possibly metamorphic origin found in the Dahongshan, Dongchuan and Hekou Groups are also indicative of such metamorphism. ~1.85 Ma mafic dykes and rapakivi granites (or A-type) in the northern Yangtze Block (Xiong et al., 2009; Peng et al., 2009; Zhang et al., 2011), and ~1.7 Ga rifting basins and mafic within-plate magmatism in the western Yangtze Block were thus thought to related to the initial fragmentation of the Columbia supercontinent (Zhao et al., 2010).

7.5.1. Comparison of detrital zircon age spectra with other cratons in Columbia

In terms of detrital zircon age spectra, late Paleoproterozoic strata in the SW Yangtze Block are most comparable to those in the Australian and North China Cratons (Fig. 14) (also see Fig. 9 of Wang et al., 2012a), although the peaks of each age spectrum among those three cratons are not well correlated with each other.

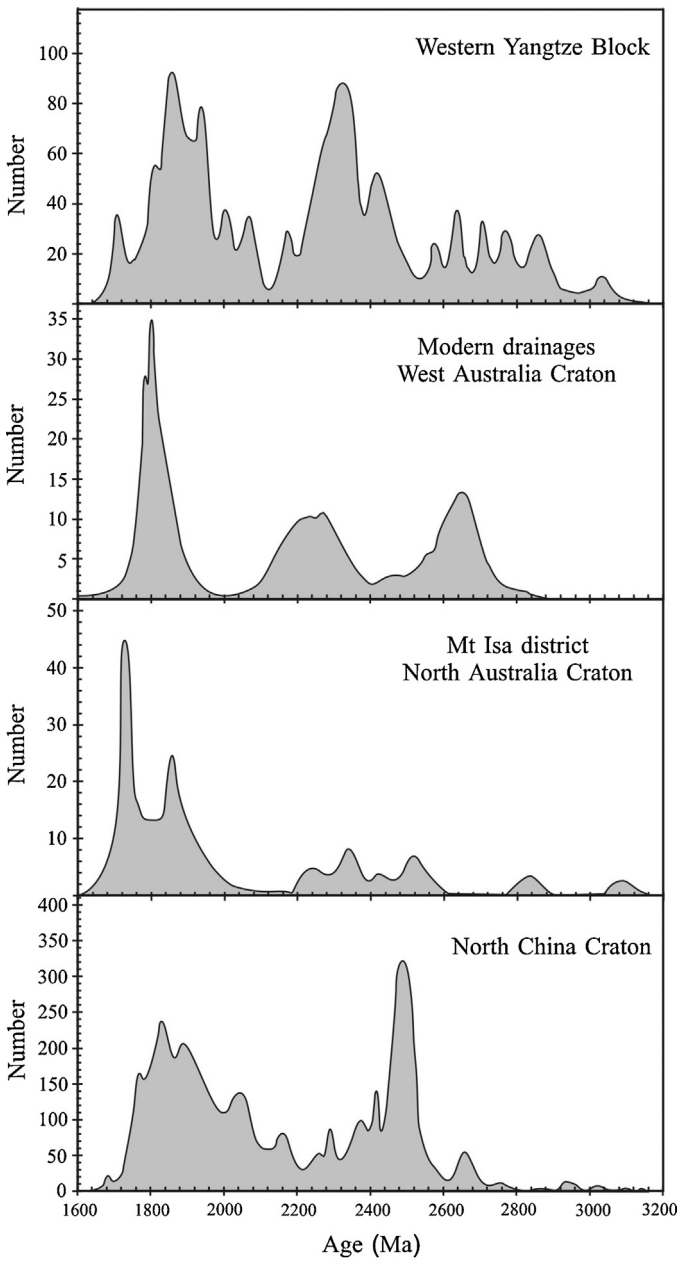

Fig. 14. Histograms of compiled concordant detrital zircon U-Pb ages between 1700 and 3200 Ma in the western Yangtze Block and different cratons of Columbia. Data are from Greentree et al. (2006), Greentree and Li (2008), Zhao et al. (2010), Wang et al. (2012a), Griffin et al. (2004, 2006), Yang et al. (2009), and Condie et al. (2009).

However, it indicates that only the Australian and North China Cratons have tectonic events that are roughly contemporaneous with those of 2.05–1.95, 2.36–2.16, 2.50–2.45 and 2.9–2.7 Ga in the western Yangtze Block (Fig. 14), suggestive of a possible link between these cratons. For example, the North China Craton contains ~2.5 Ga TTG gneisses and 2.9–2.8 Ga meta-igneous rocks (Zhai and Liu, 2003; Zhao et al., 2008a, 2008b; Liu et al., 2009). Furthermore, the Paleoproterozoic Luliang Complex, containing 2375 Ma and 2199–2173 Ma granitoid gneisses (Zhao et al., 2008a, 2008b), are also comparable to the age population of 2360–2160 Ma in the western Yangtze Block. Similarly in Australia, detrital zircon grains from modern drainages across the Yilgarn Craton in West Australian Craton show age peaks at ~1800, ~2330 and 2800–2700 Ma (Griffin et al., 2004). Detrital zircon grains of ~1800, ~2300 and 2500–2400 Ma were also reported in the Georgetown and Mt Isa districts, North Australian Craton (Griffin et al., 2006; Murgulov et al., 2007; Bierlein et al., 2008). The distinct age spectrum of 1810–1770 Ma in the Hekou Group were not documented in the Yangtze Block, and are thus possibly correlated with the post-collisional 1815–1770 Ma granitoids and meta-volcanic rocks in the North China Craton (Wan et al., 2000; Zhao et al., 2002; Zhao and Zhou, 2009), or the 1800–1750 Ma Leichhardt superbasin in North Australian Craton (Jackson et al., 2000). It is thus suggested that the Australia or North China Cratons can be potential sources for the 1810–1770 Ma and ~2300 Ma zircon grains in the western Yangtze Block. In such a case, the Yangtze Block could be positioned in the western part of the Columbia supercontinent reconstructed by Zhao et al. (2002, 2004) (Fig. 15).

7.5.2. Comparison of ~1700 Ma within-plate mafic rocks to those in Australia and North China

Metatuff and metabasalts of the Hekou Group provide tight constraints on the timing of volcanic eruption between ~1710 and ~1680 Ma, slightly older than the mafic plutons with ages of 1710–1657 Ma. These ages suggest that the within-plate mafic magmatism in the western Yangtze Block occurred about 1700 Ma. In order to further constrain the possible connection of the Yangtze Block with Australia or North China, we compare these ~1700 Ma within-plate mafic rocks with those from other cratons.

In the North China Craton, an important record for the break-up of the North China Craton from other blocks in Columbia is the 1700–1200 Ma Zhaertai-Bayan Obo-Huade-Weichang rift zone along the northern margin of the craton (Zhao et al., 2003, 2011), which comprises metamorphosed sedimentary and volcanic assemblages (Zhou et al., 2002a). If the western Yangtze Block was connected with the northern North China Craton, onset of the break-up would be at ~1700 Ma, and produced mafic rocks in both rift zones of the two blocks at this time might have similar chemical characteristics. However, ~1700 Ma mafic rocks in the Zhaertai-Bayan Obo-Huade-Weichang rift zone have uniformly depleted in Th, U, Nb, Ta, Zr and Hf in primitive mantle-normalized spider-grams, and enriched Nd isotopic values ($\varepsilon Nd(t) = -8.5$ to -8.0) (Li et al., 2007), obviously different from those of the mafic rocks in the Hekou area.

In Australia, ~1700 m Ma intra-cratonic volcano-sedimentary basins are widespread in the Leichhardt and Calvert Superbasins in the McArthur and Mount Isa Inliers and the Etheridge Group in the Georgetown Inlier of the North Australian Craton (Fig. 15) (e.g. Jackson et al., 2000; Baker et al., 2010). The Calvert Superbasin contains dominantly bimodal volcanic rocks and clastic fluvial and shallow marine sediments with ages of 1730–1670 Ma (Betts et al., 1999, 2008 and reference therein), roughly synchronous with those of the western Yangtze Block. Moreover, the metabasalts from the Etheridge Group and the intruding meta-dolerites in the Georgetown Inlier also have comparable ages from ~1720 to ~1630 Ma (Baker et al., 2010 and reference therein). These mafic rocks have compositions typical of continental-rifting rocks (Scott et al., 2000; Baker et al., 2010). Some of them display variably depleted Nb and Ta but no Zr and Hf anomalies in the multi-elemental spider-grams, and have initial $\varepsilon Nd(t)$ values of a depleted mantle source (+2.6 to +5.3; Baker et al., 2010), similar to the mafic rocks in the Hekou area.

Similar detrital zircon age patterns and whole-rock geochemical features suggest that the Yangtze Block was more likely linked with the North Australian Craton during Paleoproterozoic (Fig. 15). Future isotopic and stratigraphic comparisons will provide more insights about this possible reconstruction of Columbia.

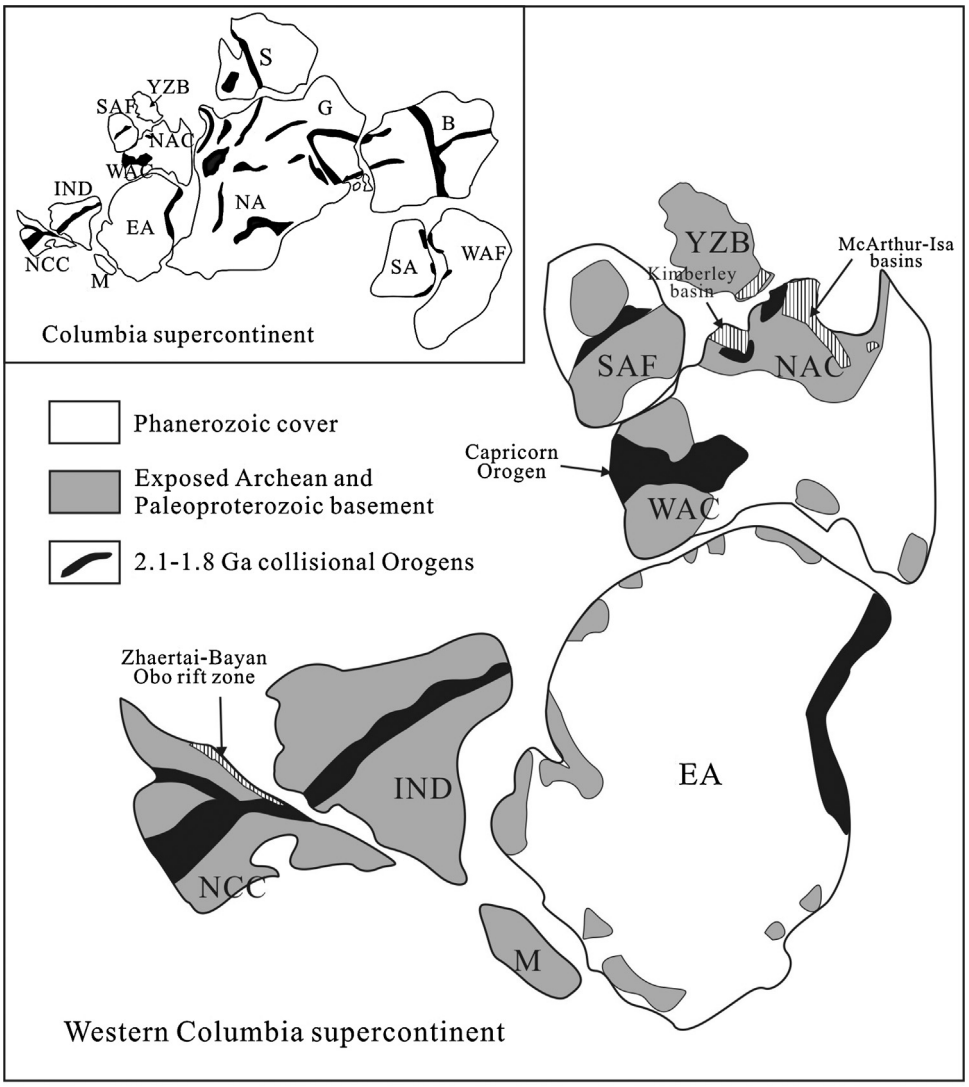

Fig. 15. Possible position of the Yangtze Block in the Columbia supercontinent reconstructed by Zhao et al. (2002).

8. Conclusions

1. Both the Hekou Group and intruding metagabbros in the western Yangtze Block have ages of about 1700 Ma. They have formed in a continental rifting setting, similar to the contemporary Dahongshan and Dongchuan Groups in the same region.
2. The Hekou Group had a Archean to Paleoproterozoic provenance which is broadly in the Yangtze Block. The 1810–1770 and 2360–2160 Ma zircon populations, poorly documented in the Yangtze Block, may represent either an exotic or now totally concealed source regions.
3. The Yangtze Block was most likely linked with the North Australian Craton in Columbia during Paleoproterozoic. The late Paleoproterozoic rift event in the western Yangtze Block can be correlated with the initial break-up of the Columbia supercontinent.

Acknowledgements

This study is supported by grants from the Research Grant Council of Hong Kong (HKU707210P and HKU707511P), and the National Natural Science Foundation of China (Grant 41272212). We thank Mr. Liang Chen and Dinghua Ma from the Lala Mine for helping with our field work. Liang Qi, Guohui Hu, Xinyu Gao and Pingping Liu are greatly appreciated for their assistances with the analyses. The manuscript has greatly benefited from constructive comments of the Editor, Peter Cawood and two anonymous reviewers.

Appendix A. Supplementary data

Supplementary data associated with this article can be found, in the online version, at http://dx.doi.org/10.1016/j.precamres.2013.03.011.

References

Amelin, Y., Lee, D.-C., Halliday, A.N., Pidgeon, R.T., 1999. Nature of the Earth's earliest crust from hafnium isotopes in single detrital zircons. Nature 399, 252–255.
Baker, M.J., Crawford, A.J., Withnall, I.W., 2010. Geochemical, Sm-Nd isotopic characteristics and petrogenesis of Paleoproterozoic mafic rocks form the Georgetown Inlier, north Queensland: implications for relationship with the Broken Hill and Mount Isa Eastern Succession. Precambrian Research 177, 39–54.
Betts, P.G., Lister, G.S., Pound, K.S., 1999. Architecture of a Paleoproterozoic rift system: evidence from the Fiery Creek Dome region, Mount Isa terrane. Australian Journal of Earth Sciences 46, 533–554.
Betts, P.G., Giles, D., Schaefer, B.F., 2008. Comparing 1800–1600 Ma accretionary and basin processes in Australia and Laurentia: possible geographic concentrations in Columbia. Precambrian Research 166, 81–92.
Bierlein, F.P., Black, L.P., Hergt, J., Mark, G., 2008. Evolution of pre-1.8 Ga basement rocks in the western Mt Isa Inlier, northeastern Australia—insights from SHRIMP

U–Pb dating and in-situ Lu-Hf analysis of zircons. Precambrian Research 163, 159–173.
Blichert-Toft, J., Albarede, F., 1997. The Lu-Hf isotope geochemistry of chondrites and the evolution of the mantle-crust system. Earth and Planetary Science Letters 148 (1–2), 243–258.
Chen, Z.L., Chen, S.Y., 1987. On the tectonic evolution of the west margin of the Yangzi Block: Chongqing, China. Chongqing Publishing House 172 (in Chinese with English abstract).
Chen, G.W., Xia, B., 2001. Study on the genesis of the Lala copper deposit, Sichuan Province: bulletin of mineralogy. Petrology and Geochemistry 20, 42–44 (in Chinese with English abstract).
Chen, W.T., Zhou, M.F., 2012. Paragenesis, stable isotopes and molybdenite Re-Os isotopic age of the Lala iron-copper deposit, Southwest China. Economic Geology 107, 459–480.
Condie, K.C., Belousova, E., Griffin, W.L., Sircombe, K.N., 2009. Granitoid events in space and time: constraints from igneous and detrital zircon age spectra. Gondwana Research 15, 228–242.
Gao, S., Qiu, Y.M., Ling, W.L., McNaughton, N.J., Groves, D.I., 2001. Single zircon U-Pb dating of the Kongling high-grade metamorphic terrain: evidence for >3.2 Ga old continental crust in the Yangtze craton. Science China Series D 4, 326–335.
Geng, Y.S., Yang, C.H., Du, L.L., Wang, X.S., Ren, L.D., Zhou, X.W., 2007. Chronology and tectonic environment of the Tianbaoshan Formation: new evidence from zircon SHRIMP U-Pb age and geochemistry. Geological Review 53, 556–563 (in Chinese with English abstract).
Greentree, M.R., Li, Z.X., 2008. The oldest known rocks in south-western China: SHRIMP U-Pb magmatic crystallization age and detrital provenance analysis of the Paleoproterozoic Dahongshan Group. Journal of Asian Earth Sciences 33, 289–302.
Greentree, M.R., Li, Z.X., Li, X.H., Wu, H.C., 2006. Late Mesoproterozoic to earliest Neoproterozoic basin record of the Sibao orogenesis in western South China and relationship to the assembly of Rodinia. Precambrian Research 151, 79–100.
Griffin, W.L., Pearson, N.J., Belousova, E., Jackson, S.E., van Achterbergh, E., Reilly, S.Y., Shee, S.R., 2000. The Hf isotope composition of cratonic mantle: LAM–MC–ICPMS analysis of zircon megacrysts in kimberlites. Geochimica et Cosmochimica Acta 64 (1), 133–147.
Griffin, W.L., Belousova, E.A., Shee, S.R., Pearson, N.J., O'Reilly, S.Y., 2004. Archean crustal evolution in the northern Yilgarn Craton: U-Pb and Hf-isotope evidence from detrital zircons. Precambrian Research 131, 231–282.
Griffin, W.L., Belousova, E.A., Walters, S.G., O'Reilly, S.Y., 2006. Archean and Proterozoic crustal evolution in the eastern succession of the Mt Isa district Australia: U-Pb and Hf-isotope studies of detrital zircons. Australia Journal of Earth Sciences 53, 125–149.
Guan, J.L., Zheng, L.L., Lui, J.H., Sun, Z.M., Cheng, W.H., 2011. Zircons SHRIMP U-Pb dating of diabase from Hekou, Sichuan Province, China and its geological significance. Acta Geologica Sinica 85 (4), 482–490 (in Chinese with English abstract).
He, D.F., Zhong, H., Zhu, W.G., Xiao, F., 2010. Geochemical characteristics of the ore-bearing strata metasedimentary host rocks in the Lala copper deposit, Sichuan province. Earth Science Frontier 17, 218–226 (in Chinese with English abstract).
Horton, B.K., Parra, M., Saylor, J.E., Nie, J., Mora, A., Torres, V., Stockli, D.F., Strecker, M.R., 2010. Resolving uplift of the northern Andes using detrital zircon age signatures. GSA Today 20 (7), 4–9.
Hu, A., Zhu, B., Mao, C., Zhu, N., Hunang, R., 1991. Geochronology of the Dahongshan Group. Chinese Journal of Geochemistry 10 (3), 195–203.
Jackson, M.J., Scott, D.L., Rawling, D.J., 2000. Stratigraphic framework for the Leichhardt and Calvert Superbasins: review and correlations of the pre-1700Ma successions between Mount Isa and McArthur River. Australian Journal of Earth Sciences 47, 381–405.
Li, F.H., Tan, J.M., Shen, Y.L., Yu, F.X., Zhou, G.F., Pan, X.N., Li, X.Z., 1988. The Presinian in the Kangdian Area. Chongqing Publishing House, Chongqing, China, 396 p. (in Chinese with English abstract).
Li, Z.X., Li, X.H., Kinny, P.D., Wang, J., Zhang, S., Zhou, H., 2003. Geochronology of Neoproterozoic syn-rift magmatism in the Yangtze Craton, South China and correlations with other continents. Evidence for a mantle superplume that broke up Rodinia. Precambrian Research 122, 85–109.
Li, X.H., Li, Z.X., Wingate, M.T.D., Chung, S.L., Liu, Y., Lin, G.C., Li, W.X., 2006. Geochemistry of the 755Ma MundineWell dyke swarm, northwestern Australia: part of a Neoproterozoic mantle superplume beneath Rodinia? Precambrian Research 146, 1–15.
Li, Q.L., Chen, F.K., Guo, J.H., Li, X.H., Yang, Y.H., Siebel, W., 2007. Zircon ages and Nd-Hf isotopic composition of the Zhaertai Group (Inner Mongolia): evidence for early Proterozoic evolution of the northern North China Craton. Journal of Asian Earth Sciences 30, 573–590.
Ling, W.L., Gao, S., Zhang, B.R., Zhou, L., Xu, Q.D., 2001. The recognizing of ca. 1.95 Ga tectono-thermal eventin Kongling nucleus and its significance for the evolution of Yangtze Block, South China. Chinese Science Bulletin 46 (4), 326–329.
Liu, Y.S., Hu, Z.C., Gao, S., Gunther, D., Xu, J., Gao, C.G., Chen, H.H., 2008. In situ analysis of major and trace elements of anhydrous minerals by LA–ICP–MS without applying an internal standard. Chemical Geology 257, 34–43.
Liu, D.Y., Wilde, S.A., Wan, Y.S., Wang, S.Y., Valley, J.W., Kita, N., Dong, C.Y., Xie, H.Q., Yang, C.X., Zhang, Y.X., Gao, L.Z., 2009. Combined U-Pb, hafnium and oxygen isotope analysis of zircons from meta-igneous rocks in the southern North China Craton reveal multiple events in the Late Mesoarchean-Early Neoarchean. Chemical Geology 261, 140–154.
Ludwig, K.R., 2003. Isoplot 3. 00: A Geochronological Toolkit for Microsoft Excel. Berkeley Geochronology Center, Berkeley, CA.
Meschede, M., 1986. A method of discrimination between different types of mid-oceanic ridge basalts and continental tholeiites with the Nb-Zr-Y diagram. Chemical Geology 56, 207–218.
Murgulov, V., Beyer, E., Griffin, W.L., O'Reilly, S.Y., Walters, S.G., Stephens, D., 2007. Crustal evolution in the Georgetown Inlier, Queensland, Australia: a detrital zircon study. Chemical Geology 245, 198–215.
Myrow, P.M., Hughes, N.C., Goodge, J.W., Fanning, C.M., Williams, I.S., Peng, S., Bhargava, O.N., Parcha, S.K., Pogue, K.R., 2010. Extraordinary transport and mixing of sediment across Himalayan central Gondwana during the Cambrian-Ordovician. Geological Society of America Bulletin 122, 1660–1670.
Pearce, J.A., 1996. Trace element geochemistry of volcanic rocks: applications for massive sulphide exploration. In: Wyman, D.A. (Ed.), A User's Guide to Basalt Discrimination Diagrams, vol. 12. Geological Association of Canada, pp. 79–113 (Short Course Notes).
Pearce, J.A., Cann, J.R., 1973. Tectonic setting of basic volcanic rocks using determined using trace element analysis. Earth and Planetary Science Letter 19, 290–300.
Pearce, J.A., Norry, M.J., 1979. Petrogenetic implications of Ti, Zr, Y, and Nb variations in volcanic rocks. Contributions to Mineralogy and Petrology 69, 33–47.
Peng, M., Wu, Y.B., Wang, J., Jiao, W.F., Liu, X.C., Yang, S.H., 2009. Paleoproterozoic mafic dyke from Kongling terrain in the Yangtze Craton and its implication. Chinese Sciences Bulletin 54 (6), 1098–1104.
Qiu, Y.M., Gao, S., McNaughton, N.J., Groves, D.I., Ling, W., 2000. First evidence of >3.2 Ga continental crust in the Yangtze craton of South China and its implications for Archean crustal evolution and Phanerozoic tectonics. Geology 28 (1), 11–14.
Ran, C.Y., Zhang, Z.J., Liu, W.H., He, M.Q., Chen, H.S., 1994. Rifting cycle and store-eyed texture of copper deposits and their geochemical evolution in Kangdian region. Science in China Series B 24, 325–330 (in Chinese).
Ritter, J.R.R., Jordan, M., Christensen, U.R., Achauer, U., 2001. A mantle plume below the Eifil volcanic fields, Germany. Earth and Planetary Science Letters 186, 7–14.
Rogers, J.J.W., Santosh, M., 2002. Configuration of Columbia, a Mesoproterozoic supercontinent. Gondwana Research 5 (1), 5–22.
Rogers, N., Macdonald, R., Fitton, J.G., George, R., Smith, M., Barreiro, B., 2000. Two mantle plumes beneath the East African rift system: Sr, Nd, and Pb isotope evidence from Kenya Rift basalts. Earth and Planetary Science Letters 176, 387–400.
SBGMR (Sichuan Bureau of Geology and Mineral Resources), 1991. Regional Geology of Sichuan Province, Geological Memoirs 23. Geological Publishing House, Beijing, China (in Chinese with English summary).
Scott, D.L., Rawlings, D.J., Page, R.W., Tarlowski, C.Z., Idnurm, M., Jackson, M.J., Southgate, P.N., 2000. Basement framework and geodynamic evolution of the Palaeoproterozoic superbasins of north-central Australia: an integrated review of geochemical, geochronological and geophysical data. Australian Journal of Earth Sciences 47, 341–380.
Söderlund, U., Patchett, P.J., Vervoort, J.D., Isachsen, C.E., 2004. The ^{176}Lu decay constant determined by Lu-Hf and U-Pb isotope systematics of Precambrian mafic intrusions. Earth and Planetary Science Letters 219 (3–4), 311–324.
Sun, S.S., McDonough, W.F. (Eds.), 1989. Magmatism in the Ocean Basins, vol. 42. Geological Society Special Publication.
Sun, M., Chen, N., Zhao, G., Wilde, S.A., Ye, K., Guo, J., Chen, Y., Yuan, C., 2008. U–Pb Zircon and Sm–Nd isotopic study of the Huangtuling granulite, Dabie-Sulu belt, China: implication for the Paleoproterozoic tectonic history of the Yangtze Craton. American Journal of Sciences 308 (4), 469–483.
Sun, W.H., Zhou, M.F., Gao, J.F., Yang, Y.H., Zhao, X.F., Zhao, J.H., 2009. Detrital zircon U-Pb geochronological and Lu-Hf isotopic constraints on the Precambrian magmatic and crustal evolution of the western Yangtze Block, SW China. Precambrian Research 172, 99–126.
Wan, T., 2004. A Summary of Tectonic Evolution of China. Geological Publishing House, Beijing, 387pp. (in Chinese with English abstract).
Wan, Y.S., Geng, Y.S., Shen, Q.H., Zhang, R.X., 2000. Khondalite series—geochronology and geochemistry of the Jiehekou Group in the Luliang area, Shanxi Province. Acta Petrology Sinica 16, 49–58 (in Chinese with English abstract).
Wang, W., Wang, F., Chen, F., Zhu, X., Xiao, P., Siebel, W., 2010. Detrital zircon ages and Hf-Nd isotopic composition of neoproterozoic sedimentary rocks in the Yangtze Block: constraints on the deposition age and provenance. The Journal of Geology 118, 79–94.
Wang, L.J., Yu, J.H., Griffin, W.L., O'Reilly, S.Y., 2012a. Early crustal evolution in the western Yangtze Block: evidence from U-Pb and Lu-Hf isotopes on detrital zircons from sedimentary rocks. Precambrian Research 222–223, 368–385.
Wang, W., Zhou, M.-F., Yan, D.-P., Li, J.-W., 2012b. Depositional age, provenance, and tectonic setting of the Neoproterozoic Sibao Group, southeastern Yangtze Block, South China. Precambrian Research 192–195, 107–124.
Winchester, J.A., Floyd, P.A., 1977. Geochemical discrimination of different magma series and their differentiation products using immobile elements. Chemical Geology 20, 325–343.
Wood, D.A., 1980. The application of a Th-Hf-Ta diagram to problems of tectono-magmatic classification and to establishing the nature of crust contamination of basaltic lavas of the British Tertiary volcanic province. Earth and Planetary Science Letters 50, 11–30.
Wu, M.D., Duan, J.S., Song, X.L., Chen, L., Dan, Y., 1990. Geology of Kunyang Group in Yunnan Province. Scientific Press of Yunnan Province, Kunming, 265 (in Chinese with English abstract).
Wu, J.M., Huang, Y.P., Liu, Z.C., 1998. Formations and ore-controlling characteristics of the marine volcanic rocks on the western margin of the Yangtze Platform: mineral deposits 17, 321–329 (in Chinese with English abstract).

Wu, Y.B., Zheng, Y.F., Gao, S., Jiao, W.F., Liu, Y.S., 2008. Zircon U-Pb age and trace element evidence for Paleoproterozoic granulite-facies metamorphism and Archean crustal rocks in the Dabie Orogen. Lithos 101 (3–4), 308–322.

Xiao, Y.F., Sun, Y., 1992. The petrologic characteristics and metamorphic pre-existing rocks of the ore-bearing rock formation in Lala copper deposits. Journal of Chengdu College of Geology 19 (2), 41–49 (in Chinese with English abstract).

Xiong, Q., Zheng, J.P., Yu, C.M., Su, Y.P., Tang, H.Y., Zhang, Z.H., 2009. Zircon U-Pb age and Hf isotope of Quanyishang A-type granite in Yichang: signification for the Yangtze continental cratonization in Paleoproterozoic. Chinese Science Bulletin 54 (3), 436–446.

Yang, J., Gao, S., Chen, C., Tang, Y.Y., Yuan, H.L., Gong, H.J., Xie, S.W., Wang, J.Q., 2009. Episodic crustal growth of North China as revealed by U-Pb age and Hf isotopes of detrital zircons from modern rivers. Geochimica et Cosmochimica Acta 73, 2660–2673.

Yuan, H.L., Gao, S., Dai, M.N., Zong, C.L., Günther, D., Fontaine, G.H., Liu, X.M., Diwu, C.R., 2008. Simultaneous determinations of U-Pb age, Hf isotopes and trace element compositions of zircon by excimer laser-ablation quardrupole and multiple-collector ICP–MS. Chemical Geology 247, 100–118.

Zhai, M.G., Liu, W.J., 2003. Palaeoproterozoic tectonic history of the North China craton: a review. Precambrian Research 122, 183–199.

Zhang, S.B., Zheng, Y.F., Wu, Y.B., Zhao, Z.F., Gao, S., Wu, F.Y., 2006a. Zircon U-Pb age and Hf-O isotope evidence for Paleoproterozoic metamorphic event in South China. Precambrian Research 151 (3–4), 265–288.

Zhang, S.B., Zheng, Y.F., Wu, Y.B., Zhao, Z.F., Gao, S., Wu, F.Y., 2006b. Zircon U-Pb age and Hf isotope evidence for 3.8 Ga crustal remnant and episodic reworking of Archean crust in South China. Earth and Planetary Science Letter 252 (1–2), 56–71.

Zhang, L.J., Ma, C.Q., Wang, L.X., She, Z.B., Wang, S.M., 2011. Discovery of Paleoproterozoic rapakivi granite on the northern margin of the Yangtze block and its geological significance. Chinese Science Bulletin 56 (3), 306–318.

Zhao, J.H., Zhou, M.F., 2007. Neoproterozoic adakitic plutons and arc magmatism along the western margin of the Yangtze Block, South China. Journal of Geology 115, 675–689.

Zhao, T.P., Zhou, M.F., 2009. Geochemical constraints on the tectonic setting of Paleoproterozoic A-type granites in the southern margin of the North China Craton. Journal of Asian Earth Sciences 36, 183–195.

Zhao, X.F., Zhou, M.F., 2011. Fe-Cu deposits in the Kangdian region, SW China: a Proterozoic IOCG (iron-oxide-copper-gold) metallogenic province. Mineralium Deposita 46, 731–747.

Zhao, G., Cawood, P.A., Wilde, S.A., Sun, M., 2002. Review of global 2.1–1.8 Ga orogens: implications for a pre-Rodinia supercontinent. Earth-Sciences Reviews 59 (1–4), 125–162.

Zhao, G., Sun, M., Wilde, S.A., Li, S., 2003. Assembly, accretion and breakup of the Paleo-Mesoproterozoic Columbia supercontinent: records in the North China Craton. Gandwana Research 6 (3), 417–434.

Zhao, G., Sun, M., Wilde, S.A., Li, S., 2004. A Paleo-Mesoproterozoic supercontinent: assembly, growth and breakup. Earth-Sciences Reviews 67, 91–123.

Zhao, G., Wilde, S.A., Sun, M., Li, S., Li, X., Zhang, J., 2008a. SHRIMP U-Pb zircon ages of granitoid rocks in the Luliang complex: implications for the accretion and evolution of the Trans-North China Orogen. Precambrian Research 160, 213–226.

Zhao, J.H., Zhou, M.F., Yan, D.P., Yang, Y.H., Sun, M., 2008. Zircon Lu-Hf isotopic constraints on Neoproterozoic subduction-related crustal growth along the western margin of the Yangtze Block, China. Precambrian Research 163, 189–209.

Zhao, X.F., Zhou, M.F., Li, J.W., Sun, M., Gao, J.F., Sun, W.H., Yang, J.H., 2010. Late Paleoproterozoic to early Mesoproterozoic Dongchuan Group in Yunnan, SW China: implications for tectonic evolution of the Yangtze Block. Precambrian Research 182, 57–69.

Zhao, G., Li, S., Sun, M., Wilde, S.A., 2011. Assembly, accretion and breakup of the Paleo-Mesoproterozoic Columbia supercontinent: records in the North China Craton revisited. International Geology Review 53 (11–12), 1331–1356.

Zhou, J.Y., 2005. The geochemical characteristics and continental geodynamics of Lala copper deposit. Unpublished Ph.D thesis, The Chengdu University of Technology, Chengdu, China, pp. 20–27 (in Chinese with English abstract).

Zhou, J.B., Zheng, Y.E., Yang, X.Y., Su, Y., Wei, C.S., Xie, Z., 2002a. Tectonic framework and evolution of the Bayan Obo area. Geological Journal of China Universities 8, 46–61 (in Chinese with English abstract).

Zhou, M.-F., Yan, D.-P., Kennedy, A.K., Li, Y., Ding, J., 2002b. SHRIMP U-Pb zircon geochronological and geochemical evidence for Neoproterozoic arc-magmatism along the western margin of the Yangtze Block, South China. Earth Planet and Science Letter 196, 51–67.

Zhou, M.-F., Ma, Y., Yan, D.-P., Xia, X., Zhao, J.H., Sun, M., 2006. The Yanbian Terrane (Southern Sichuan Province, SW China): a Neoproterozoic arc assemblage in the western margin of the Yangtze Block. Precambrian Research 144, 19–38.